Redox Biology 70 (2024) 103038

Contents lists available at ScienceDirect

Redox Biology

journal homepage: www.elsevier.com/locate/redox

Endothelial H_2S-AMPK dysfunction upregulates the angiocrine factor PAI-1 and contributes to lung fibrosis

Xiangqi Chen [a], Han Wang [a], Chuan Wu [a], Xiaoyan Li [a], Xiaojuan Huang [a], Yafeng Ren [a], Qiang Pu [b], Zhongwei Cao [a], Xiaoqiang Tang [a,**], Bi-Sen Ding [a,*,1]

[a] Key Laboratory of Birth Defects and Related Diseases of Women and Children of MOE, State Key Laboratory of Biotherapy, NHC Key Laboratory of Chronobiology, Development and Related Diseases of Women and Children, Key Laboratory of Sichuan Province, West China Second University Hospital, Sichuan University, Chengdu, 610041, China

[b] Department of Thoracic Surgery, National Frontier Center of Disease Molecular Network, West China Hospital, Sichuan University, Chengdu, 610041, China

ARTICLE INFO

Keywords:
Lung fibrosis
Vascular endothelial cells
AMPK
H_2S
PAI-1
YAP

ABSTRACT

Dysfunction of the vascular angiocrine system is critically involved in regenerative defects and fibrosis of injured organs. Previous studies have identified various angiocrine factors and found that risk factors such as aging and metabolic disorders can disturb the vascular angiocrine system in fibrotic organs. One existing key gap is what sense the fibrotic risk to modulate the vascular angiocrine system in organ fibrosis. Here, using human and mouse data, we discovered that the metabolic pathway hydrogen sulfide (H_2S)-AMP-activated protein kinase (AMPK) is a sensor of fibrotic stress and serves as a key mechanism upregulating the angiocrine factor plasminogen activator inhibitor-1 (PAI-1) in endothelial cells to participate in lung fibrosis. Activation of the metabolic sensor AMPK was inhibited in endothelial cells of fibrotic lungs, and AMPK inactivation was correlated with enriched fibrotic signature and reduced lung functions in humans. The inactivation of endothelial AMPK accelerated lung fibrosis in mice, while the activation of endothelial AMPK with metformin alleviated lung fibrosis. In fibrotic lungs, endothelial AMPK inactivation led to YAP activation and overexpression of the angiocrine factor PAI-1, which was positively correlated with the fibrotic signature in human fibrotic lungs and inhibition of PAI-1 with Tiplaxtinin mitigated lung fibrosis. Further study identified that the deficiency of the antioxidative gas metabolite H_2S accounted for the inactivation of AMPK and activation of YAP-PAI-1 signaling in endothelial cells of fibrotic lungs. H_2S deficiency was involved in human lung fibrosis and H_2S supplement reversed mouse lung fibrosis in an endothelial AMPK-dependent manner. These findings provide new insight into the mechanism underlying the deregulation of the vascular angiocrine system in fibrotic organs.

1. Introduction

Fibrosis is a chronic and progressive medical condition due to dysregulated connective tissue repair response. Various organs and tissues can develop fibrosis, including skin, heart, kidney, liver, and lung. The combined annualized incidence of fibrosis-related diseases is about 4968 per 100,1000 person-years [1]. Approximately 45% of all deaths in developed countries are caused by fibrosis [2], indicating an unmet clinical need. Lung fibrosis, a consequence of chronic lung injury, can lead to compromised gas exchange, dyspnea, and diminished quality of life [3]. Only two drugs, Pirfenidone and Nintedanib, have been approved by the US Food and Drug Administration (FDA) in 2014 for the treatment of the fibrotic lung disease, idiopathic pulmonary fibrosis (IPF) [2,4,5]. However, these two drugs can only improve lung function and slow down the progression of lung fibrosis, but cannot reverse fibrotic lungs. Hence, in-depth research on the pathogenesis of lung fibrogenesis is essential to identify specific diagnostic biomarkers and therapeutic targets.

In addition to epithelial cell injury/senescence and uncontrolled activation/proliferation of fibroblasts, immune and vascular cells also participate in organ fibrosis [6]. Endothelial cells, lining the lumen of blood vessels, are not only passive conduits for delivering blood to

* Corresponding author.
** Corresponding author.
E-mail addresses: tangxiaoqiang@scu.edu.cn (X. Tang), dingbisen@scu.edu.cn (B.-S. Ding).
[1] Lead contact and senior author.

https://doi.org/10.1016/j.redox.2024.103038
Received 21 November 2023; Received in revised form 28 December 2023; Accepted 10 January 2024
Available online 11 January 2024

transport oxygen and nutrients throughout the body but are also recognized as specialized niche cells secreting angiocrine factors, such as plasminogen activator inhibitor type-1 (PAI-1), Jagged 1, Thrombospondin-1 (TSP-1), and metallopeptidase 14 (MMP14) [7–11]. Previous studies aimed to identify individual angiocrine factors and explore their functions in tissue regeneration and fibrosis. Tissue-specific endothelial cells produce specific angiocrine factors that regulate blood coagulation, inflammatory cell trafficking, metabolic homeostasis, and tissue development. Notably, angiocrine factors from endothelial cells are indispensable for guiding responses to regeneration and fibrosis [12,13]. In fibrotic livers, vascular endothelial cells produce extracellular vesicles, containing angiocrine factors Insulin-like growth factor–binding protein 7 (IGFBP7) and ADAMTS1, to enrich fibrogenic T_H17 cells [14]. For lung fibrosis, endothelial dysfunction and vascular remodeling also lead to regenerative defects and promote fibrosis [7,12,15,16]. Our previous studies have also shown that lung capillary endothelial cells produce MMP14 to promote the proliferation of epithelial progenitor cells for alveologenesis and activate CXC chemokine receptor (CXCR7) to protect against epithelial damage after injury [10,16,17]. In addition to the identification of angiocrine factors, previous studies from our lab and others have also found the effects of fibrotic risk factors, such as aging and metabolic disorders, on the deregulation of the angiocrine system and the facilitation of tissue fibrosis [13,18–22]. Thus, identifying the key responders that sense fibrotic risk to modulate the vascular angiocrine system in organ fibrosis is urgently needed and could offer new therapeutic options for fibrotic lung diseases.

Growing evidence supports the notion that endothelial function is critically regulated by its metabolic pattern [23,24], and metabolic regulators can modulate endothelial identity and biological functions such as angiogenesis [25–27]. The key metabolic regulator is AMP-activated protein kinase (AMPK), a vital cellular energy sensor and regulator that controls the shift from anabolic to catabolic metabolism. In mammals, AMPK comprises catalytic α-subunits and regulatory β-subunits, γ-subunits [28]. Upon changes in the ATP-to-AMP ratio, AMPK is activated by phosphorylation of the α-subunit. AMPK is involved in multiple pathological processes including cancer, obesity, diabetes, and fibrosis [29–32]. An increasing number of studies have found that AMPK modulates the response of endothelial cells to various diseases including endothelial function and phenotype transition [33–37]. For instance, AMPK regulates endothelial angiotensin-converting enzyme 2 (ACE2) phosphorylation at S680 to increase its stability and maintain eNOS-derived nitric oxide bioavailability, endowing endothelial cells with lung hypertension-protective phenotype [36–38]. Endothelial-specific AMPK activation protects endothelial progenitor cell function against diabetes-induced impairment and reendothelialization by the induction of heme oxygenase-1 [39]. AMPK activation also protects the vascular endothelium against chronic systemic inflammation, such as atherosclerosis [40,41]. These facts highlight the pivotal role of AMPK in regulating endothelial homeostasis and prompted us to explore whether the metabolic orchestrator AMPK serves as a sensor to regulate the vascular angiocrine system in fibrotic lungs.

Here, with multiple layers of evidence, we demonstrated that the dysfunction of the metabolic pathway hydrogen sulfide (H_2S)-AMPK is a key mechanism upregulating the angiocrine factor PAI-1 in endothelial cells and participates in lung fibrosis of humans and mice. This study provides new insights into the dysregulated vascular angiocrine system in fibrotic lungs.

2. Materials and methods

2.1. Human samples and ethical approval

Fibrotic (n = 5) and control (n = 5) lung tissues were collected at the West China Hospital, Sichuan University. This study was approved by the Medical Ethics Committee of the West China Hospital of Sichuan University.

2.2. Mice

The *Prkaa1*$^{loxP/loxP}$ mice (Stock No: 014141) were obtained from the Jackson Laboratory. Mice expressing endothelial cell-specific VE-Cadherin-Cre^{ERT2} were kindly provided by Ralf H. Adams. Floxed *Prkaa1* (*Prkaa1*$^{loxP/loxP}$) mice were crossed with endothelial cell-specific *VE-Cadherin-Cre*^{ERT2} mice to generate *VE-Cadherin-Cre*^{ERT2};*Prkaa1*$^{loxP/loxP}$ mice. Then, *VE-Cadherin-Cre*^{ERT2};*Prkaa1*$^{loxP/loxP}$ mice and *Prkaa1*$^{loxP/loxP}$ mice were intraperitoneally injected with tamoxifen (Sigma, T5648) at a dose of 100 mg/kg for six days and interrupted for three days after the third injections to obtain endothelial-specific deletion of *Prkaa1* mice (*Prkaa1*$^{\triangle EC}$) and control mice (*Prkaa1*^{WT}). C57BL/6 wild-type mice were purchased from GemPharmatech. All animal experiments were performed according to protocols approved by the Institutional Animal Care and Use Committee of West China Second University Hospital, Sichuan University.

2.3. Animal experiments

For the lung fibrosis model, 6 to 8-week mice were intratracheally injected with bleomycin (Selleck, S1214) at a dose of 3 U/kg, whereas control mice were intratracheally injected with isopycnic saline. For the treatment of lung fibrosis, bleomycin-injured mice were intraperitoneally injected with NaHS (10 mg/kg; Sigma, 161527), metformin (100 mg/kg; Solarbio, D9351), or respective vehicle for 21 days. The PAI-1 inhibitor Tiplaxtinin (5 mg/kg; TargetMol, T2030) was administered intragastrically for 21 days.

2.4. Flow cytometry

To obtain lung endothelial cells, the lung tissues were digested with Collagenase I (Roche, 11088793001) plus Dispase II (Roche, 04942078001) at a working concentration of 2 mg/mL for 30 min at 37 °C. Red blood cells were then disintegrated using red blood lysis buffer (155 mM NH_4Cl,12 mM $NaHCO_3$, 0.1 mM EDTA). The remaining viable cells were incubated with PerCP-Cy™5.5 Anti-Mouse CD45 antibody (BD, 550994) and PE Rat Anti-Mouse CD31 antibody (BD, 553373) at 4 °C under gentle rotation for 30 min. After centrifugation, the cells were washed once with PBS containing 1% donkey serum and 2 mM EDTA. Finally, flow cytometry sorting was performed to obtain $CD45^-CD31^+$ lung endothelial cells with FACS Aria III (BD Biosciences).

2.5. Magnetic-activated cell sorting (MACS)

CD31 (BD Bioscience, 553370) or CD45 (BD Bioscience, 553076) antibodies were incubated with Dynabeads Sheep anti-Rat IgG (Invitrogen, 11035) at 4 °C overnight. Fresh lung tissues were digested and then treated with red blood lysis buffer, as described above. Single-cell suspensions were incubated with Dynabead-conjugated CD45 antibody for CD45-negative selection, followed by endothelial cell purification with Dynabead-conjugated CD31 antibody. MACS buffer (2 mM EDTA, 0.1% BSA, 1% penicillin/streptomycin/antimitotic in PBS) was used for the incubation process and for washing after antibody incubation. The final obtained pure lung endothelial cells were used immediately for the subsequent RNA and protein extraction.

2.6. Cell culture

Human umbilical vein endothelial cells (HUVECs) were isolated and cultured in Endothelial Cell Basal Medium-2 (Lonza, CC-3156) added with EGM™-2 SingleQuots™ Supplements (Lonza, CC-4176). HEK293T cells were cultured in Dulbecco's Modified Eagle Medium (HyClone, SH30023.01) supplemented with 10% FBS. HUVECs were treated with

NaHS (0.1, 1 mM), verteporfin (0.25 μM), or the control vehicle for 24 h. HUVECs were treated with NaHS (1 mM) for 24 h for qRT-PCR, or treated with TGFβ (Proteintech; 20 ng/mL) for 24 h for RNA-seq. For lentivirus construction, the targeting shRNAs (sh*PRKAA1*, 5′-GTTGCCTACCATCTCATAATA-3'; sh*YAP*, 5-CCCAGTTAAATGTTCAC-CAAT-3′) were cloned into PLKO.1 plasmid and generated in HEK293T first. Then, HUVECs were infected with lentivirus carrying sh*PRKAA1*, sh*YAP*, or negative control. Puromycin (1 μg/mL) was used to screen successfully infected cells after 48 h. For knockdown of *MPST* by siRNA, si*MPST* (si*MPST*-1#, 5′-AGAGTGTTTCTTCACTCAA-3'; si*MPST*-2#, 5′-AGACCTACGAGGACATCAA-3′) or negative control were transfected into HUVECs with Lipofectamine RNAiMAX (Invitrogen, 13778150) for 48 h.

2.7. Immunostaining, histological analysis, and H_2S measurement

Fresh mouse lung tissues and human lung tissues were embedded in OCT and stored at -80 °C. Then, tissues were cut into 6 μm for subsequent H_2S measurement or immunofluorescent staining. For histological analysis, fresh mouse lung tissues were fixed in 4% paraformaldehyde for 24 h, and then the fixed tissues were cut into 5 μm for H&E staining, Sirius red staining, or Masson staining. For immunofluorescent staining, tissue slices were warmed at room temperature and then washed with PBS for 5 min. Then, tissue slices were fixed in 4% paraformaldehyde for 5 min at room temperature. After two washes with PBS for every 5 min, tissue slices were blocked in PBS containing 4% donkey serum and 0.05% tween-20 for 1 h at 37 °C. Later, they were incubated with primary anti-Collagen I (Proteintech, 14695-1-AP) or anti-α-SMA (Abcam, ab7817) antibodies overnight at 4 °C. Tissue slices were washed and then incubated with Alexa Fluor 488 Donkey Anti-Rabbit IgG (Jackson, 711-545-152) or Alexa Fluor 488 Donkey Anti-Mouse IgG (Jackson,715-545-150) for 1 h at 37 °C. Then, tissue slices were washed three times and incubated with DAPI (Roche, 10236276001) for 10 min at room temperature. Finally, the slices were washed and sealed with an anti-fluorescence attenuation sealer, followed by image capture and processing using LSM980 (Zeiss) and Zen Blue (Zeiss). For H_2S measurement, the content of H_2S in lung tissue slices was monitored using Sulfidefluor 7 AM (Tocris, 4943). Freshly isolated tissue slices were loaded with Sulfidefluor 7 AM (10 μM) and incubated at 37 °C for 45 min. Then, tissue slices were washed twice with PBS, followed by DAPI staining for 5 min, and washed with PBS. Images were captured at the excitation and emission wavelengths of 495 and 520 nm, respectively.

2.8. Measurement of hydroxyproline

The hydroxyproline content in lung tissues was measured using Hydroxyproline (HYP) Assay Kit (Solarbio, BC0255). Briefly, tissues of equal weight were cut into as many pieces as possible. Then, tissues are baked overnight in 12 N hydrochloric acid at 110 °C and neutralized with sodium hydroxide. Next, the samples were added to 1.4% chloramine T in 0.5 M sodium acetate/10% isopropanol and incubated for 20 min at room temperature. Ehrlich's solution was added into samples for 30 min incubation at 65 °C. Finally, the absorbance values of all samples were measured at 560 nm, and the Hydroxyproline content was calculated based on the fresh weight of tissues and the standard curve.

2.9. Real-time quantitative PCR (RT-qPCR)

Total RNA was extracted by TRIzol reagent (Invitrogen, 15596026). PrimeScript™ RT reagent Kit (TaKaRa, RR047A) was used for cDNA synthesis. To determine the mRNA levels of the target genes, AceQ qPCR SYBR Green Master Mix (Vazyme, Q111-02) was used according to the manufacturer's instructions. The primers of target genes are shown in Table S1.

2.10. Western blot

Total protein was extracted by RIPA lysis buffer (Beyotime Biotechnology, P0013B) supplemented with protease inhibitors (Merck, HY-K0010) and phosphatase inhibitors (Bimake, B15002). The following primary antibodies are used for Western blot: AMPKα (Abcam, ab32047), *p*-AMPKα (Cell Signaling Technology, 2535S), α-SMA (Proteintech, 23660-1-AP), Collagen I (Proteintech, 14695-1-AP), CTGF (Proteintech, 23936-1-AP), PAI-1 (Proteintech, 13801-1-AP), GAPDH (Proteintech, 60004-1-Ig), YAP (Proteintech, 13584-1-AP), p-YAP (Cell Signaling Technology, 13008). Horseradish peroxidase (HRP)-conjugated Goat Anti-Rabbit IgG (H + L) and HRP-conjugated Goat Anti-Mouse IgG (H + L) from Servicebio (GB23303, GB23301) were used as secondary antibodies.

2.11. Bioinformatic analysis

Microarray and Bulk RNA-seq of mouse (GSE181508, GSE148893) or human lung tissues (GSE38958, GSE213001), ChIP-seq of HUVECs (GSE163458), single-cell RNA-seq of human IPF patient lung endothelial cells (GSE159354) are download from GEO database. Bulk RNA sequencing data that support the findings of this study have been deposited in NCBI Gene Expression Omnibus (GSE250474). For the microarray datasets, the microarray probes were converted into gene symbols using the biomaRt R package. The Spearman correlation analysis was performed to determine the correlation between *PRKAA1* expression and human lung function parameters. For bulk RNA-seq, the DEseq2 R package was used for differential analysis of count data. The results of the differential analysis were pre-ranked according to the $\log_2$FoldChange, and then enrichment analysis was performed using Gene Set Enrichment Analysis (GSEA) software. The GSVA R package was used for Gene Set Variation Analysis (GSVA). For Single-cell RNA-seq, all data were analyzed with Seurat R package. Briefly, endothelial cells from IPF patients and controls meeting the standard (min.cells = 3, min.features = 200) were used for the next normalization (NormalizeData) and finding high variable genes (FindVariableFeatures, nfeatures = 2000). Then, the "Find Integration Anchors" and "IntegrateData" functions were used to combine data and eliminate batch effects using high variable genes as input. The ggplot2 R package was used for image rendering. CHIP-seq analysis was performed as described previously [42]. Trim_galore was used for quality control and sequencing adapter elimination. Single-end sequencing data were aligned to the human genome using Bowtie2, followed by Samtools for BAM file conversion. Peak calling results were demonstrated using Integrative Genomics Viewer.

2.12. Statistical analysis

All results shown were obtained by at least three biologically independent experiments and the values are presented as means ± standard error of the mean (SEM). The Shapiro-Wilk test was applied to assess the normality of the data. The standard Student's *t*-test was applied when there were two groups with a normal distribution, while one-way ANOVA with Bonferroni *post hoc* test was applied when there were more than two groups with normal distribution. Otherwise, the Mann-Whitney *U* test was used for two groups of nonparametric analysis. For more than two groups of nonparametric analysis, we applied the Kruskal-Wallis test followed by Dunn's *post hoc* test to correct for multiple comparisons. GraphPad Prism 8.0 was used for all the statistical analysis.

3. Results

3.1. AMPK inactivation is involved in lung fibrosis in mice and humans

Considering the critical roles of the metabolic orchestrators in

regulating vascular endothelial cells, we hypothesized that dysfunction of the metabolic sensor AMPK may be a key mechanism underlying the dysfunction of the vascular angiocrine system in lung fibrosis. Thus, we analyzed the activation of the AMPK signaling pathway by reusing public RNA-seq data of endothelial cells (ECs) from mouse control and fibrotic lungs. Gene Set Enrichment Analysis (GSEA) revealed that the AMPK signaling pathway was repressed in endothelial cells of mouse fibrotic lungs compared with the control lungs (Fig. 1a). To further validate this finding, we purified endothelial cells from control and fibrotic lungs and analyzed the phosphorylation of AMPK. Indeed, the Western blot results showed that AMPK phosphorylation/activation was inhibited in endothelial cells from fibrotic lungs (Fig. 1b). Next, we tested whether the AMPK signaling pathway was also repressed in human fibrotic lungs. To this end, we analyzed the transcriptome data of human control and fibrotic lungs and observed that AMPK signature was downregulated in human fibrotic lungs (Fig. 1c), indicating that AMPK activation was inhibited in human fibrotic lungs. We subsequently explored whether AMPK inactivation was associated with lung fibrosis in human patients. Spearman correlation analysis revealed that AMPK signature was negatively correlated with fibrotic genes, including *Collagen type I alpha 1 chain* (*COL1A1*), *Collagen type III alpha 1 chain* (*COL3A1*), and *Actin alpha 2 smooth muscle* (*ACTA2*) (Fig. 1d). In

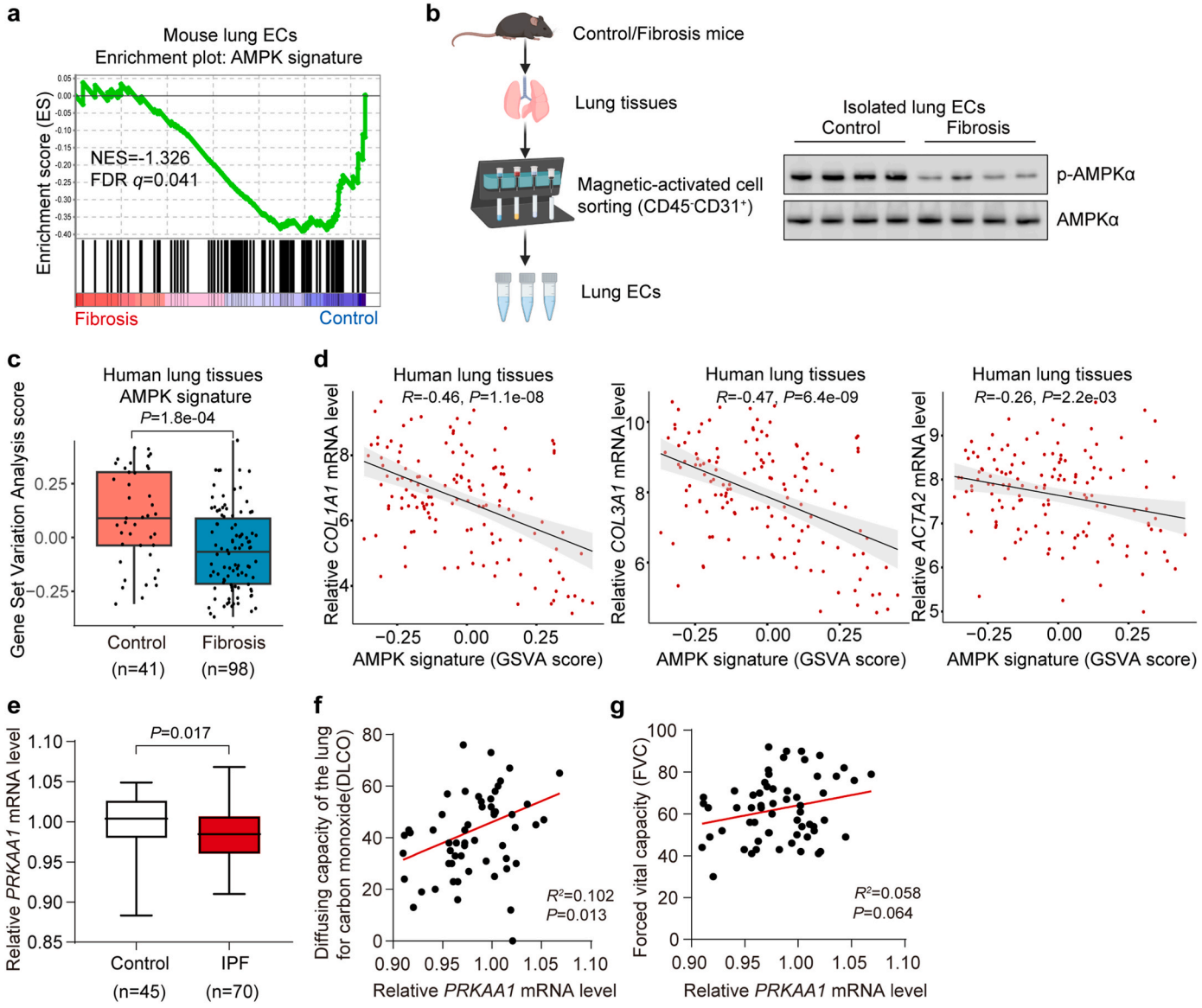

Fig. 1. AMPK is inactivated in human and mouse fibrotic lungs. (a) The AMPK signaling pathway is repressed in endothelial cells (ECs) of mouse fibrotic lungs. Transcriptome data (GSE181508) of lung endothelial cells from bleomycin-induced fibrotic lungs and control lungs were subjected to Gene Set Enrichment Analysis (GSEA) of AMPK_SIGNALING_PATHWAY. (b) AMPK phosphorylation/activation is repassed in endothelial cells of mouse fibrotic lungs. Lung fibrosis was induced by bleomycin for three weeks, then endothelial cells from fibrotic and control lungs were isolated by Magnetic-Activated Cell Sorting (MACS) with indicated antibodies ($CD45^{-}CD31^{+}$). Western blot was performed to test the phosphorylation/activation of AMPK in endothelial cells of fibrotic and control lungs. (c) The AMPK signaling pathway is repressed in human fibrotic lungs. Transcriptome data (GSE213001) of 41 control and 98 fibrotic lung samples were subjected to analyze the Gene Set Variation Analysis (GSVA) score of AMPK_SIGNALING_PATHWAY (AMPK signature). (d) AMPK signature is negatively correlated with the expression of fibrotic marker genes (*COL1A1, COL3A1, ACTA2*). Transcriptome data in (c) were subjected to Spearman correlation analysis. (e) AMPK mRNA (*PRKAA1*) is reduced in PBMCs from patients with lung fibrosis. *PRKAA1* mRNA level from 45 control donors and 70 IPF patients PBMCs using the GEO public microarray dataset GSE38958. (f–g) *PRKAA1* level is positively correlated with lung function parameters. The correlation of *PRKAA1* mRNA level with lung function in patients with lung fibrosis was performed with Spearman correlation analysis using the GSE38958 microarray dataset. DLCO, diffusing capacity for carbon monoxide; FVC, forced vital capacity.

addition, AMPK (*PRKAA1*) expression level was also decreased in peripheral blood mononuclear cells (PBMCs) from lung fibrosis patients (Fig. 1e), and *PRKAA1* expression was positively correlated with the lung function parameters: diffusing capacity of the lungs for carbon monoxide (DLCO) and forced vital capacity (FVC) (Fig. 1f and g). Therefore, these data suggested that AMPK was systemically (endothelial cells, lung tissues, and PBMCs) inactivated in both human and mouse fibrotic lungs, and AMPK inactivation was correlated with lung fibrotic markers and reduced lung function in patients.

3.2. Endothelial AMPK inactivation contributes to lung fibrosis

The aforementioned findings suggest that endothelial AMPK inactivation may contribute to lung fibrosis. Thus, we next examined whether endothelial AMPK inactivation contributed to lung fibrosis by knocking out AMPK in endothelial cells specifically. Since catalytic α-subunit of AMPK in both humans and mice have two isoforms, α1 and α2, encoded by the genes *Prkaa1* and *Prkaa2* [43]. We first analyzed the expression patterns of *Prkaa1* and *Prkaa2* in mouse lung endothelial cells and found that *Prkaa1* had much higher expression abundance than *Prkaa2* (Fig. 2a). Therefore, we chose to knock out *Prkaa1* to mimic the inhibition of AMPK activation *in vivo*. For the construction of EC-specific *Prkaa1* knockout mice, we bred *Prkaa1* floxed mice ($Prkaa1^{loxP/loxP}$) with mice expressing EC-specific inducible Cre (VE-Cadherin-Cre^{ERT2}). The offspring $Prkaa1^{loxP/loxP}$/VE-cadherin-Cre^{ERT2} and $Prkaa1^{loxP/loxP}$ mice were treated with tamoxifen to generate EC-specific *Prkaa1* knockout mice ($Prkaa1^{\triangle EC}$) and control wild-type ($Prkaa1^{WT}$) mice (Fig. 2b) [17]. We performed fluorescence-activated cell sorting (FACS) for purifying $CD45^{-}CD31^{+}$ lung ECs and validated that *Prkaa1* was significantly knocked out but the expression of *Prkaa2* was comparable in $Prkaa1^{\triangle EC}$ mice compared with the wild-type ($Prkaa1^{WT}$) mice (Fig. 2c).

To explore the roles of endothelial AMPK inactivation in lung fibrosis, $Prkaa1^{\triangle EC}$ and $Prkaa1^{WT}$ mice were then subjected to single bleomycin challenge to induce lung fibrosis (Fig. 2d). Notably, the bleomycin challenge significantly induced remodeling and collagen deposition in mouse lung tissues and endothelial AMPK inactivation promoted bleomycin-induced lung fibrosis, as revealed by hematoxylin-eosin (H&E) and picrosirius red (PSR) staining (Fig. 2e). Further immunofluorescence staining of Collagen I and alpha-smooth muscle actin (αSMA) also validated that endothelial AMPK inhibition increased extracellular matrix (ECM) deposition in fibrotic lungs (Fig. 2f). Consistently, the expression levels of fibrotic-related gene mRNA (*Col1a1*, *Col3a1*, *Ctgf*, *Fn1*) and protein (Collagen I, αSMA, CTGF) in fibrotic lungs were also aggravated by endothelial AMPK inactivation (Fig. 2g and i). Accumulation of hydroxyproline is another hallmark of fibrotic lungs [16], we also observed enhanced accumulation of hydroxyproline in fibrotic lungs with endothelial AMPK knockout compared with the wild-type mice (Fig. 2h). Thus, these data indicate that endothelial AMPK inactivation exacerbates lung fibrosis in mice.

Next, we explored whether the activation of endothelial AMPK could reverse lung fibrosis by treating mice with the well-known AMPK activator metformin (Supplementary Fig. S1a). Metformin treatment could activate endothelial AMPK in fibrotic lungs (Supplementary Fig. S1b). Accordingly, metformin decreased bleomycin-induced lung fibrosis in mice, as indicated by H&E, PSR, and Masson staining (Supplementary Fig. S1c). Therefore, endothelial AMPK inactivation contributes to lung fibrosis, and the AMPK agonist, metformin, can activate endothelial AMPK and reverse fibrosis.

3.3. AMPK regulates PAI-1 expression via the YAP signaling pathway in endothelial cells

We next sought to unravel the mechanism by which endothelial AMPK regulates lung fibrosis. To this end, we knocked down *PRKAA1* in human umbilical vein endothelial cells (HUVECs) (Supplementary Fig. S2a). The effects of *PRKAA1* knockdown on the transcriptome of endothelial cells were analyzed using bulk RNA-seq. GSEA was performed to analyze the HALLMARK gene sets, and we noticed the enrichment of fibrosis-associated HALLMARK gene sets in human endothelial cells with *PRKAA1* knockdown (Fig. 3a; Supplementary Fig. S2b). Interestingly, the intersection of the five pivotal HALLMARK gene sets identified two common genes, *F3* and *SERPINE1*, and only *SERPINE1* was significantly upregulated following *PRKAA1* knockdown in human endothelial cells (Fig. 3b). The *SERPINE1* gene encodes plasminogen activator inhibitor-1 (PAI-1), a member of the serine-protease inhibitor superfamily with important roles in tissue fibrosis [44–46]. Thus, we proposed that endothelial AMPK may regulate lung fibrosis *via* the anti-fibrinolytic factor PAI-1. To this end, we first explored whether and how AMPK regulates PAI-1 expression in endothelial cells. Consistent with the RNA-seq results, qRT-PCR results showed that *SERPINE1* mRNA expression was upregulated after *PRKAA1* knockdown in human endothelial cells (Fig. 3c). To explore the potential involvement of endothelial PAI-1 in endothelial cells in lung fibrosis, we analyzed endothelial *SERPINE1* expression in mouse and human fibrotic lungs. *Serpine1* mRNA expression was significantly upregulated in endothelial cells of mouse fibrotic lungs compared with the control lungs (Fig. 3d). Consistently, the *SERPINE1* expression level was also significantly upregulated in endothelial cells of human fibrotic lungs (Fig. 3e). The upregulation of PAI-1 in endothelial cells of mouse and human fibrotic lungs may be due to the inactivation of AMPK because we observed that PAI-1 was upregulated in bleomycin-treated $Prkaa1^{\triangle EC}$ mice compared with $Prkaa1^{WT}$ mice (Fig. 3f). Collectively, these data suggest that PAI-1 is a key downstream factor of AMPK in endothelial cells, and endothelial PAI-1 levels are reduced in endothelial cells of fibrotic lungs in humans and mice.

Then we explored how AMPK regulates PAI-1 expression in endothelial cells during lung fibrosis. AMPK regulates multiple important signaling pathways in cells. One such pivotal signaling pathway is the Hippo pathway. The Hippo/YAP pathway is involved in tissue injury, fibrosis, and repair by controlling the transcriptional events [47]. AMPK inhibits the Hippo/YAP pathway *via* multiple direct mechanisms during metabolic stress [48–50]. We tested whether the Hippo pathway was involved in AMPK-mediated repression of PAI-1 in endothelial cells. First, we validated the regulation of Hippo by AMPK in endothelial cells of fibrotic lungs because the Hippo effector YAP was hyperactivated/hypophosphorylation in lung endothelial cells with *Prkaa1* knockout (Fig. 3g). Activated YAP translocates to the nucleus to cooperate with TAZ as a transcriptional cofactor to initiate translational events of their target genes by binding directly to promoters [47]. To explore whether YAP regulates *SERPINE1* expression directly, we analyzed the binding of YAP and its partners, TAZ and TEAD1, to the promoter of *SERPINE1* in human endothelial cells using public ChIP-seq data (Fig. 3h). Indeed, YAP and its partners can bind to the promoter of *SERPINE1*, suggesting that the AMPK downstream factor YAP may regulate *SERPINE1* expression directly. We observed that shRNA-mediated knockdown of *YAP* and verteporfin-mediated inhibition of YAP suppressed *SERPINE1* expression in human endothelial cells (Fig. 3i–k). Thus, AMPK inactivation resulted in the activation of YAP in endothelial cells from fibrotic lungs, leading to the transcription of the angiocrine factor *SERPINE1* (PAI-1) (Fig. 3l).

3.4. PAI-1 contributes to lung fibrosis in human and mouse

The angiocrine factor PAI-1 participates in tissue remodeling in both coagulation-dependent and -independent manners [46,51]. The roles of PAI-1 in the fibrosis of different organs are contradictory [45,46], and the roles of PAI-1 in lung fibrosis are not fully understood. Therefore, we investigated the role of PAI-1 in human and mouse lung fibrosis. We analyzed the correlation between *SERPINE1* level and fibrotic marker genes in human fibrotic lungs using a public dataset (GSE213001). The Spearman correlation analysis revealed that *SERPINE1* expression level

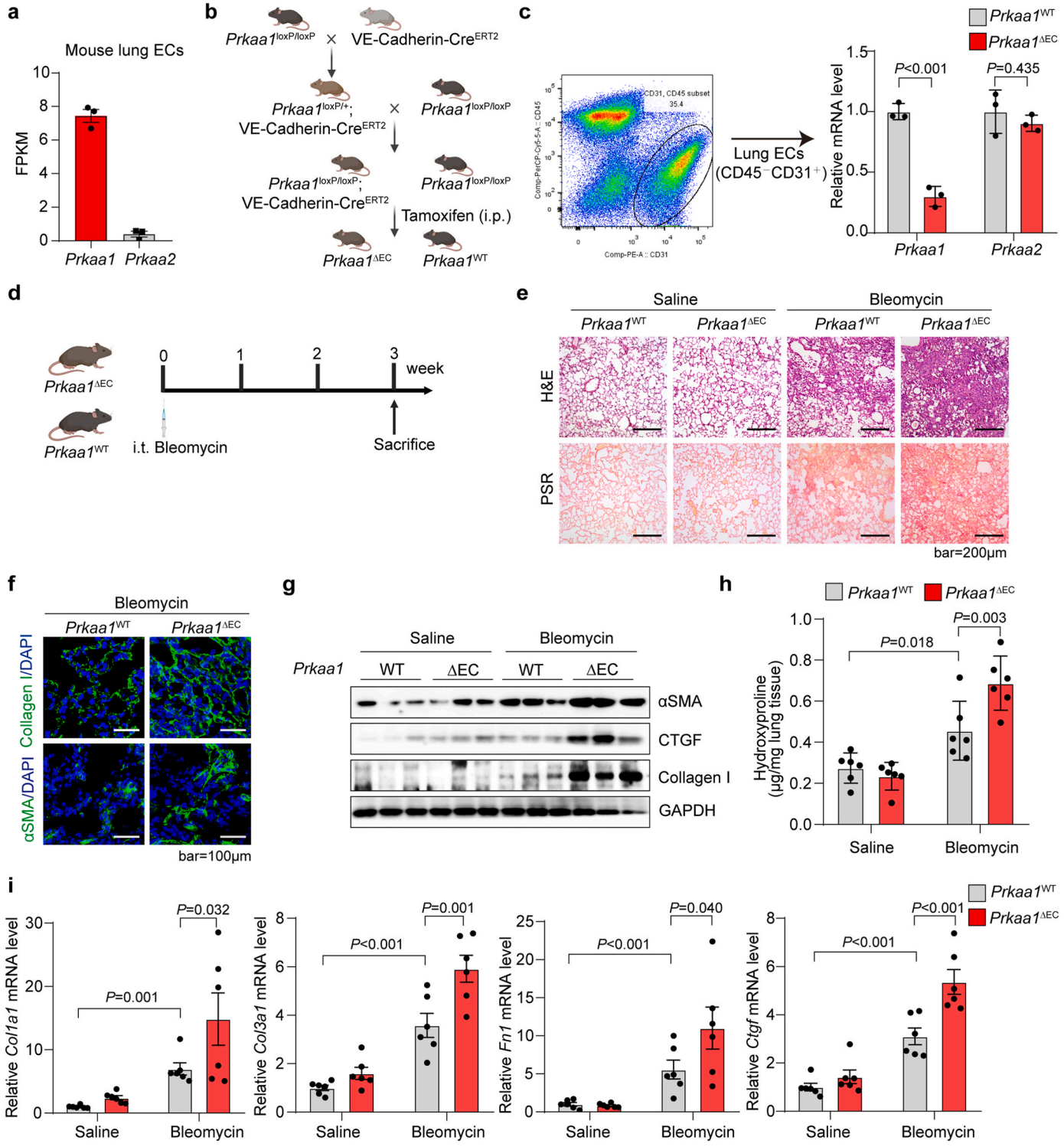

Fig. 2. Endothelial cell-specific *Prkaa1* knockout promotes lung fibrosis. (a) FPKM value of *Prkaa1* and *Prkaa2* in mouse lung ECs showing higher expression abundance of *Prkaa1* (n = 3). Bulk RNA-seq data of mouse lung ECs was downloaded from the GEO database (GSE148893). (b) Schematic diagram for generating endothelial-specific *Prkaa1* knockout mice. (c) Validation of *Prkaa1* knockout efficacy in lung endothelial cells. Lung endothelial cells ($CD45^{-}CD31^{+}$) were purified from $Prkaa1^{WT}$ and $Prkaa1^{\triangle EC}$ mice with FACS, followed by qRT-PCR analysis of *Prkaa1* and *Prkaa2* mRNA levels (n = 3). (d) Schematic diagram showing mouse lung fibrosis model. Lung fibrosis was induced in $Prkaa1^{WT}$ and $Prkaa1^{\triangle EC}$ mice by intratracheal injection with bleomycin. (e) H&E and PSR staining showing increased remodeling and collagen deposition in $Prkaa1^{\triangle EC}$ mice compared with $Prkaa1^{WT}$ in bleomycin-induced fibrotic lungs. (f) Immunofluorescent staining of Collagen and alpha-smooth Muscle Actin (αSMA) showing increased extracellular matrix in $Prkaa1^{\triangle EC}$ mice compared with $Prkaa1^{WT}$. (g) Expression of fibrosis-related proteins (αSMA, CTGF, Collagen I) is increased in $Prkaa1^{\triangle EC}$ mice lung tissue compared with $Prkaa1^{WT}$. (h) Measurement of hydroxyproline content in lung tissues from $Prkaa1^{\triangle EC}$ and $Prkaa1^{WT}$ mice (n = 6). (i) Measurement of fibrosis-related genes (*Col1a1*, *Col3a1*, *Ctgf*, *Fn1*) mRNA level in $Prkaa1^{\triangle EC}$ and $Prkaa1^{WT}$ mice lung tissues (n = 6).

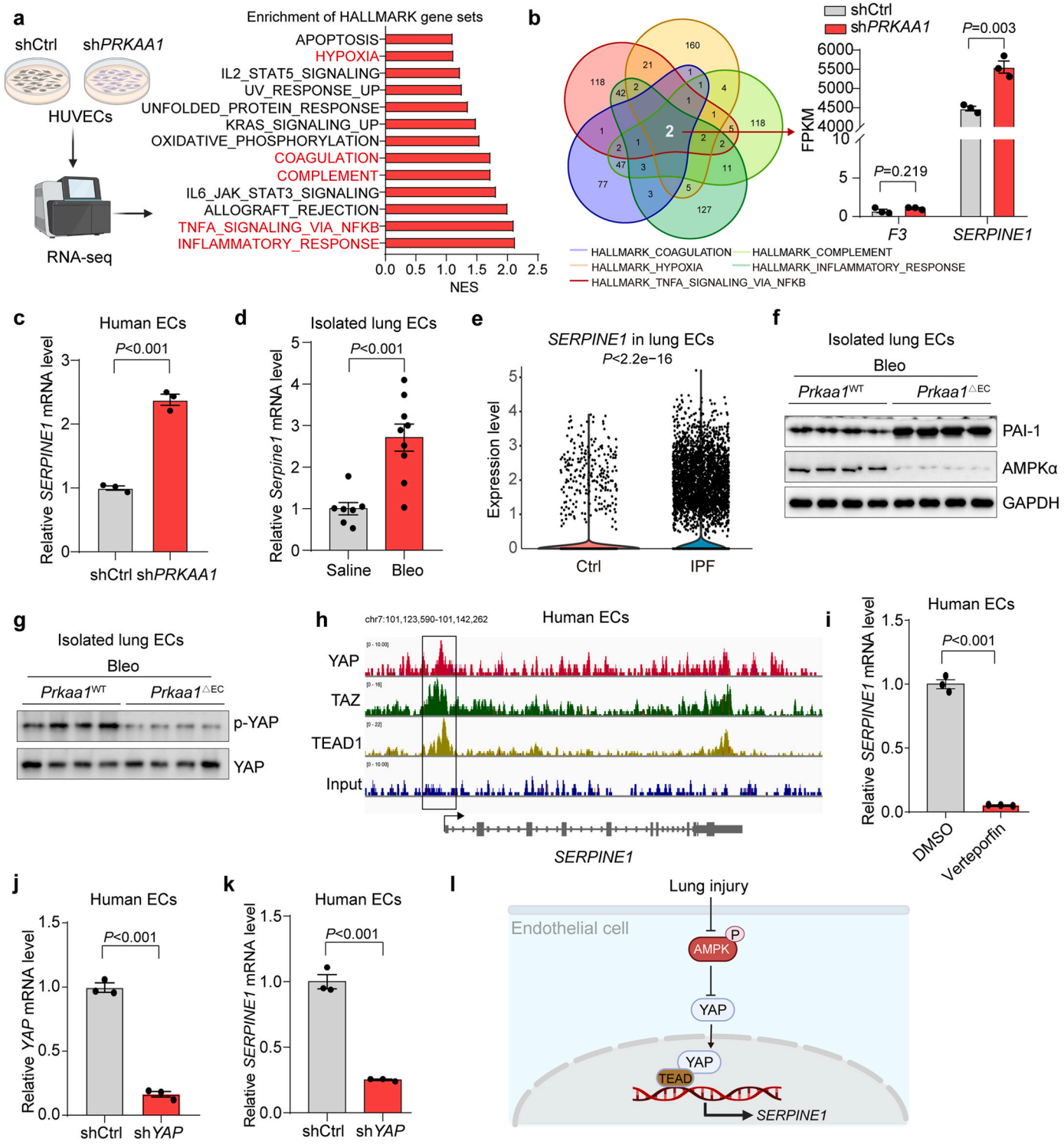

(caption on next page)

Fig. 3. AMPK regulates PAI-1 expression through YAP in endothelial cells in fibrotic lungs. (a) AMPK regulates fibrosis-associated hallmarks in endothelial cells. *PRKAA1* was silenced in HUVECs by lentivirus-mediated shRNA, followed by TGFβ treatment for 24 h. Then, HUVECs were collected for bulk RNA-seq, followed by gene set enrichment analysis (GSEA) of HALLMARK gene sets. The top enriched HALLMARK gene sets in endothelial cells with AMPK deficiency are shown. (b) *SERPINE1* is a key downstream gene of AMPK in human endothelial cells. The intersection of key HALLMARK gene sets from a (red) identified *F3* and *SERPINE1* as two core genes in the key HALLMARK gene sets, and AMPK effects on the expression values (FPKM) of *F3* and *SERPINE1* are shown. (c) *PRKAA1* knockdown increases *SERPINE1* expression in human endothelial cells. HUVECs were treated as in (a), followed by qRT-PCR analysis of *SERPINE1* mRNA level (n = 3). (d) *Serpine1* expression is increased in endothelial cells from mouse fibrotic lungs. Mouse lung fibrosis was induced by bleomycin (Bleo), lung endothelial cells were purified with the MACS method and followed qRT-PCR analysis of *Serpine1* expression in lung ECs from control (Saline) or fibrotic (Bleo) lungs (Saline, n = 7; Bleo, n = 9). (e) Violin plot showing increased *SERPINE1* expression in lung ECs from human fibrotic lungs compared with control lungs. scRNA-seq data of human lung fibrosis (GSE159354) was downloaded from the GEO database, and the transcriptome of lung endothelial cells was analyzed. (f) *Prkaa1* knockout upregulates *Serpine1* (PAI-1) in endothelial cells from mouse fibrotic lungs. (g) *Prkaa1* knockout activates YAP (reduced phosphorylation) in endothelial cells from mouse fibrotic lungs. (h) ChIP-Seq profiling of HUVECs showing YAP, TAZ, and TEAD1 binding to the promoter region of *SERPINE1*. GSE163458 ChIP-Seq data was downloaded from the GEO database. (i) Inhibition of YAP with verteporfin inhibits *SERPINE1* expression in human endothelial cells. HUVECs were treated with YAP inhibitor verteporfin (0.25 μM) for 48 h, followed by qRT-PCR analysis of *SERPINE1* (n = 3). (j–k) Knockdown of *YAP* reduces *SERPINE1* expression in human endothelial cells. HUVECs were infected with lentivirus carrying shCtrl or sh*YAP* for 48 h, followed by qRT-PCR analysis of *YAP* and *SERPINE1* levels (n = 3). (l) Schematic diagram for AMPK-YAP-PAI-1 axis in endothelial cells of fibrotic lungs. (For interpretation of the references to colour in this figure legend, the reader is referred to the Web version of this article.)

was positively correlated with the mRNA levels of fibrotic genes (*COL1A1*, *COL3A1*, *CCN2*, *FN1*) (Fig. 4a). These findings suggested that PAI-1 is potentially involved in lung fibrosis. To validate this finding, we inhibited PAI-1 using Tiplaxtinin (TPX) in mice with lung fibrosis (Fig. 4b). TPX treatment diminished lung tissue remodeling and collagen deposition in fibrotic lungs, as evidenced by H&E and PSR staining (Fig. 4c). Immunofluorescence staining of Collagen I and αSMA also showed that TPX decreased ECM deposition in fibrotic lungs (Fig. 4d). Consistently, fibrotic genes expression (*Col1a1*, *Col3a1*, *Ctgf*, *Fn1*) were downregulated in mouse fibrotic lungs treated with TPX (Fig. 4e), indicating the profibrotic role of PAI-1 in mouse lung fibrosis. Overall, endothelial AMPK inactivation induces PAI-1 upregulation, which contributes to lung fibrosis, and the PAI-1 inhibitor TPX can reverse lung fibrosis in mice.

3.5. Dysregulated H_2S-AMPK promotes PAI-1 expression via the Hippo/YAP pathway in ECs

The aforementioned results demonstrated that AMPK inactivation promotes YAP activation and PAI-1 overexpression in endothelial cells, which facilitates the development of lung fibrosis. One major question is how endothelial AMPK is inhibited in fibrotic lungs. AMPK acts as a metabolic sensor. Its activation is critically regulated by ATP/AMP and other metabolites that regulate the ATP/AMP ratio. Endothelial cells are key sources and targets of gaseous metabolites. One such metabolite is endogenous hydrogen sulfate (H_2S), which regulates the ATP/AMP ratio to activate AMPK by targeting the mitochondrial respiratory chain [52,53]. H_2S is a critical oxidant scavenger ameliorating vascular metabolic stress and vascular adaptation [52,54–56], which may rely on the activation effects of H_2S on AMPK [52,53]. Therefore, we tested whether H_2S could regulate the AMPK-YAP-PAI-1 signaling axis in endothelial cells. We found that H_2S donor NaHS activated AMPK and induced YAP phosphorylation (inactivation) in human endothelial cells (Fig. 5a). H_2S donor also inhibited *SERPINE1* expression in human endothelial cells, which was abolished by *PRKAA1* knockdown (Fig. 5b and c), suggesting that H_2S can regulate *SERPINE1* expression in an AMPK-dependent manner in endothelial cells. In mammalian cells, the gas metabolite H_2S is naturally synthesized by three key enzymes, including cystathionine γ-lyase (CTH), cystathionine β-synthetase (CBS), and mercaptopyruvate sulfurtransferase (MPST) [57]. Among these three synthetases, *MPST* showed the highest expression in endothelial cells (Fig. 5d). Thus, we designed two siRNAs to knockdown *MPST* to mimic H_2S deficiency (Fig. 5e), and tested the effects of MPST/H_2S deficiency on AMPK-YAP-PAI-1 signal in endothelial cells. In contrast to H_2S supplementation, *MPST* knockdown inhibited AMPK activation and resulted in YAP hyperactivation in human endothelial cells (Fig. 5f), which was consistent with the upregulation of *SERPINE1* expression in human endothelial cells following *MPST* knockdown (Fig. 5g).

Next, we explored whether H_2S deficiency correlated with PAI-1 expression and lung fibrosis in humans. To this end, we reanalyzed the scRNA-seq data of human control and fibrotic lungs and observed the reduction of endothelial *MPST* in human fibrotic lungs (Fig. 5h), which was coupled with H_2S deficiency in fibrotic lungs (Fig. 5i). Besides, we also observed that *MPST* was negatively correlated with *SERPINE1* in human fibrotic lungs (Fig. 5j).

Collectively, the dysfunction of the AMPK-YAP-PAI-1 axis in endothelial cells of fibrotic lungs may be due to the downregulation of MPST and the deficiency of endogenous H_2S.

3.6. H_2S alleviates lung fibrosis in an endothelial AMPK-dependent manner

Since the endogenous H_2S was decreased in fibrotic lungs, we examined the correlation between the expression of H_2S synthetase MPST and the expression of fibrosis-related genes. Spearman correlation analysis showed that *MPST* expression was negatively correlated with the expression of fibrosis-related genes (*COL1A1*, *COL3A1*, *CCN2*, *FN1*) in human fibrotic lungs (Fig. 6a), indicating that H_2S deficiency may contribute to lung fibrosis.

Finally, we tested whether H_2S regulated lung fibrosis *via* endothelial AMPK. To this end, H_2S donor NaHS was intraperitoneally injected daily to treat bleomycin-induced lung fibrosis in *Prkaa1*$^{\triangle EC}$ and *Prkaa1*^{WT} mice (Fig. 6b). In fibrotic lungs of wild-type mice, H_2S supplement decreased remodeling and collagen deposition (Fig. 6c), deposition of Collagen I and αSMA (Fig. 6d), accumulation of hydroxyproline (Fig. 6e), and expression of fibrotic marker genes (*Col1a1*, *Col3a1*, *Ctgf*, *Fn1*) (Fig. 6f). Notably, the effects of H_2S in repressing lung fibrosis was abolished by endothelial AMPK knockout because H_2S cannot repress lung fibrosis in *Prkaa1*$^{\triangle EC}$ mice (Fig. 6b–f). Thus, H_2S suppresses lung fibrosis in an endothelial AMPK-dependent manner.

Overall, H_2S deficiency is correlated with lung fibrosis in humans, and supplementation with H_2S can reduce lung fibrosis in mice, which depends on endothelial AMPK activation.

4. Discussion

Decoding the cellular and molecular mechanisms of the vascular niche in fibrosis might help us elucidate how the vascular ecosystem contributes to organ homeostasis. Previous studies have identified several angiocrine factors from endothelial cells in organ fibrosis and have demonstrated that risk factors such as aging and metabolic disorders can regulate angiocrine factors to facilitate organ fibrosis. However, one of the key questions is which signal senses risk factors to regulate angiocrine factors in endothelial cells to participate in organ fibrosis. Here, we provide evidence that endothelial AMPK senses the deficiency of endogenous H_2S during fibrotic stress, which leads to the

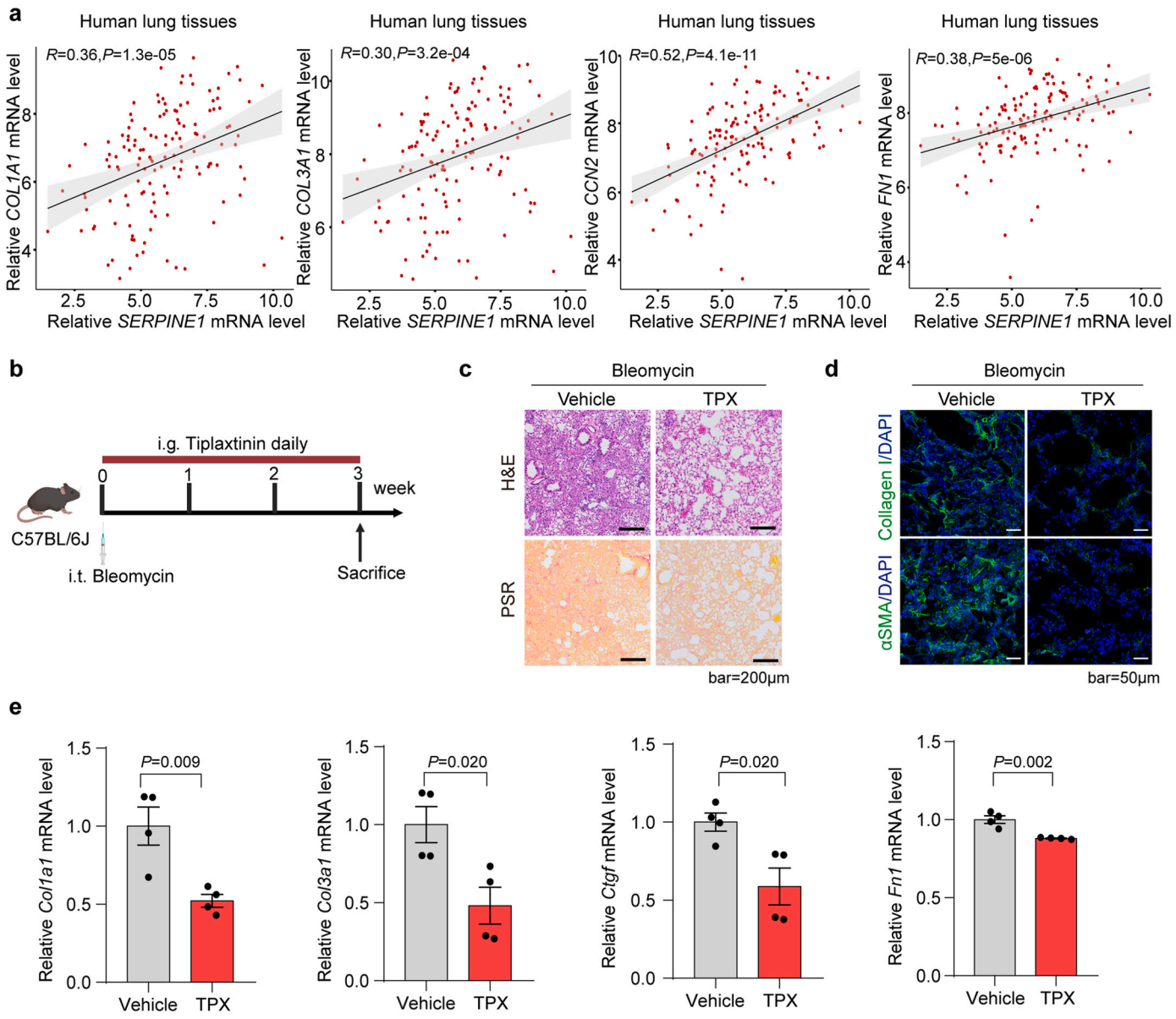

Fig. 4. PAI-1 participates in lung fibrosis in humans and mice. (a) *SERPINE1* mRNA expression is positively correlated with fibrotic markers. Bulk RNA-seq data of 41 human control lung tissues and 98 fibrotic lung tissues (GSE213001) was used to analyze the correlation of *SERPINE1* and the expression of fibrotic marker genes (*COL1A1*, *COLA3A1*, *CCN2*, *FN1*) with Spearman correlation analysis. (b) Design of PAI-1 inhibitor treatment of mouse lung fibrosis. Mouse lung fibrosis was induced by bleomycin, followed by PAI-1 inhibitor (Tiplaxtinin; 5 mg/kg/day; i.g.) for 21 days. (c) H&E and PSR staining reveal that Tiplaxtinin (TPX) reduces tissue remodeling and collagen deposition in fibrotic lungs. (d) Immunofluorescent staining reveals that Tiplaxtinin decreases Collagen and αSMA expression in fibrotic lungs. (e) qRT-PCR analysis reveals that Tiplaxtinin decreases the expression of fibrotic marker genes (*Col1a1*, *Col3a1*, *Ctgf*, *Fn1*) in fibrotic lungs (n = 4).

upregulation of the angiocrine factor PAI-1 and aggravates lung fibrosis (Fig. 7). These findings may fill the gaps in our understanding of how intracellular responders sense risk factors to regulate angiocrine factors in organ fibrosis.

Metabolic dysregulation is a vital pathogenic process involved in fibrosis. Metabolic regulators such as AMPK, FOXOs, and HIFs are critically involved in organ fibrosis. For instance, the metabolic sensor AMPK has been shown to participate in various tissue fibrosis, including non-alcoholic steatohepatitis (NASH), cardiac and lung fibrosis [31,32,58,59]. However, previous studies have been limited to the tissue level and have not focused on the activity and role of AMPK in specific cell types, such as vascular cells. Here, we showed that AMPK is inactivated in endothelial cells of fibrotic lungs. Importantly, we observed a systemic reduction in AMPK activation and provided evidence that AMPK inactivation was correlated with enhanced fibrotic signatures and reduced lung functions. Deficiency of endothelial AMPK promotes lung fibrosis in mice, whereas the AMPK activator, metformin, can activate endothelial AMPK and repress lung fibrosis. Thus, AMPK-mediated metabolic homeostasis may be critical for the anti-fibrotic function of endothelial cells in the lungs. Together with previous findings in other types of lung cells [32,60,61], our findings suggested that AMPK activators, such as metformin, can serve as potential anti-fibrotic drugs.

Indeed, the AMPK activation is critical for endothelial homeostasis and its anti-fibrotic function. The activation of AMPK is critically regulated by the ATP/AMP ratio and other metabolites that regulate this ratio. As a specific cell type, endothelial cells are an important source and target of gas metabolites such as NO, CO, and H_2S. Among these metabolites, the rising star H_2S is an essential endogenous gaseous transmitter involved in many biological functions, such as molecular signaling cascade activation, protein post-translational modification,

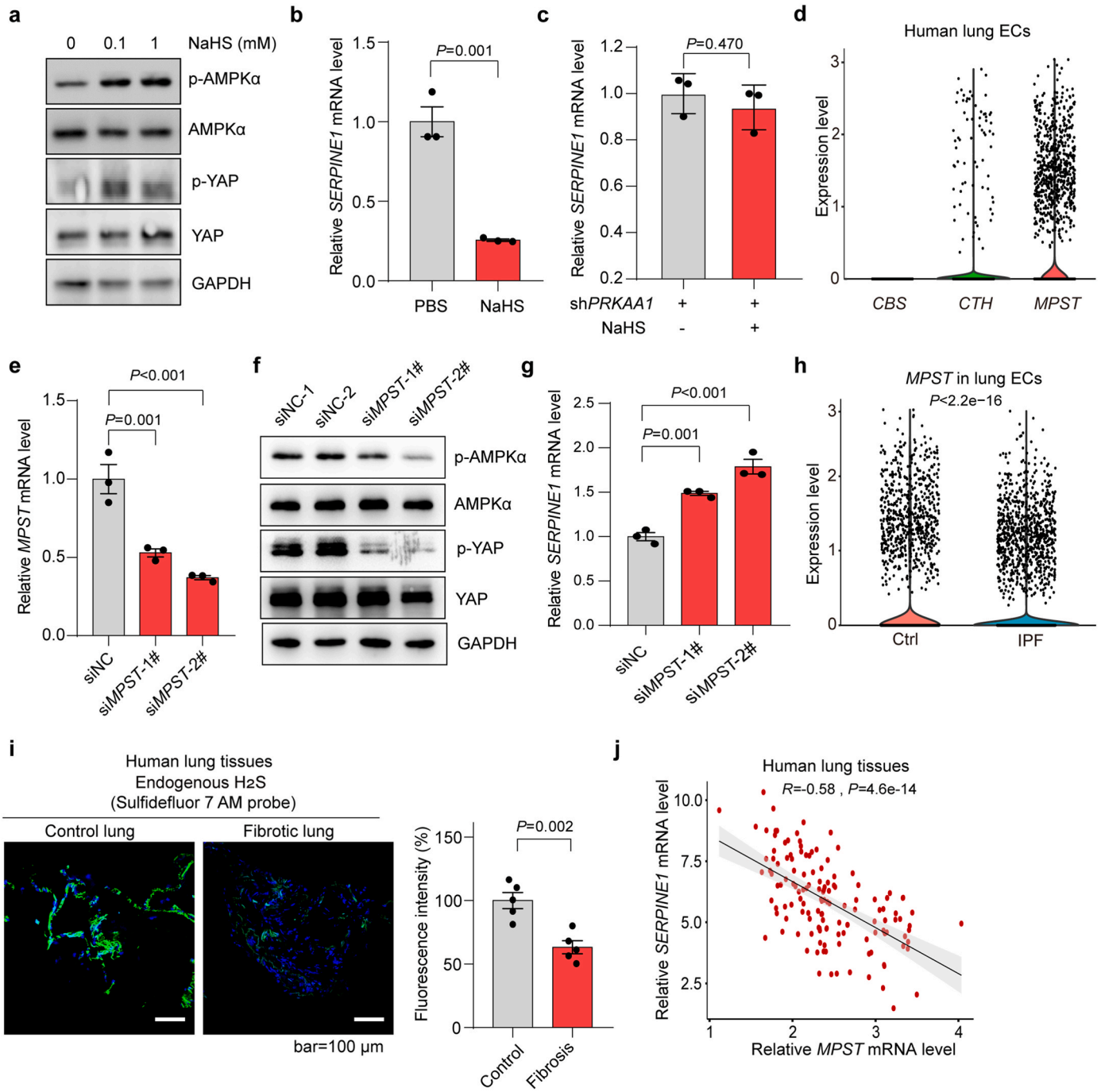

Fig. 5. Hydrogen sulfide regulates the AMPK-YAP-PAI-1 axis in endothelial cells. (a) Hydrogen sulfide (H_2S) donor NaHS induces AMPK activation and YAP phosphorylation/inactivation in human endothelial cells. HUVECs were treated with/without NaHS for 24 h, followed by Western blot analysis of AMPK and YAP activation. (b) H_2S donor NaHS inhibits *SERPINE1* expression in human endothelial cells. HUVEC cells were treated with NaHS (1 mM) for 24 h, followed by qRT-PCR analysis of *SERPINE1* expression (n = 3). (c) *PRKAA1* knockdown counteracts the inhibitory effect of H_2S on *SERPINE1* expression in human endothelial cells. HUVECs were infected with lentivirus carrying sh*PRKAA1* and treated with NaHS (1 mM) for an additional 24 h, followed by qRT-PCR analysis of *SERPINE1* expression (n = 3). (d) Expression levels of the three H_2S synthetases (*CBS*, *CTH*, *MPST*) in human lung ECs. Transcriptome data of human lung endothelial cells were obtained from the public dataset GSE159354. (e) siRNA-mediated knockdown of *MPST* in human endothelial cells. HUVECs were transfected with si*MPST* or siNC for 24 h, followed by qRT-PCR analysis of *MPST* mRNA level (n = 3). (f) Knockdown of *MPST* inhibits AMPK activation and YAP phosphorylation/inactivation in human endothelial cells. HUVECs were treated as in (e). (g) Knockdown of *MPST* increases the expression of *SERPINE1* in human endothelial cells. HUVECs were treated as in (e) (n = 3). (h) Expression of the key H_2S synthetase MPST is reduced in endothelial cells from human fibrotic lungs. The transcriptome of endothelial cells from fibrotic and control lung tissues was analyzed with the public scRNA-seq dataset GSE159354. (i) H_2S level is reduced in human fibrotic lungs. Endogenous H_2S in human fibrotic and control lungs were detected with the probe Sulfidefluor 7 AM (n = 5). (j) *MPST* expression is negatively correlated with *SERPINE1* in human lung tissues. The Spearman correlation analysis of *SERPINE1* mRNA expression level with *MPST* mRNA expression level in human lung tissues was performed using the public dataset GSE213001.

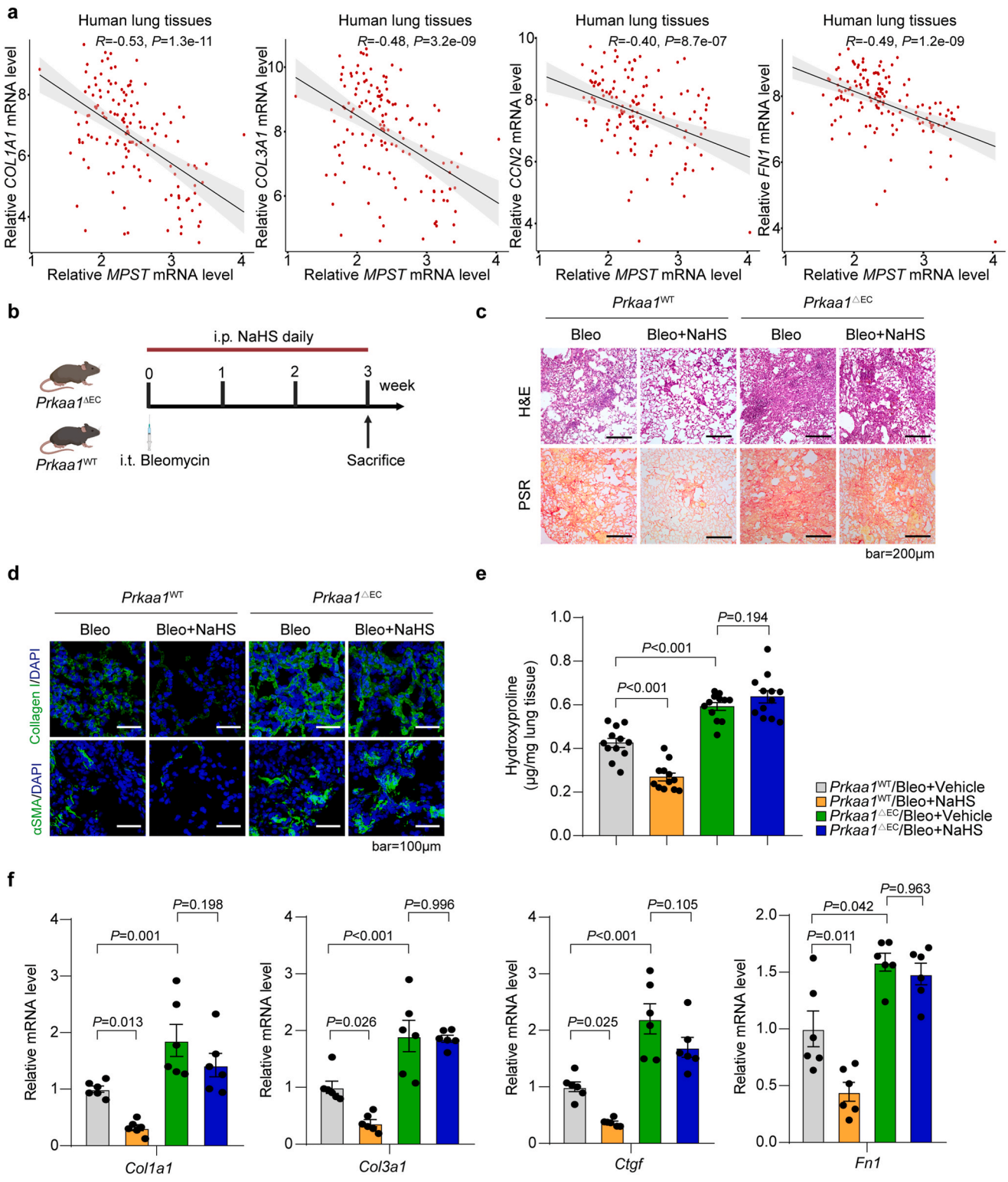

Fig. 6. Hydrogen sulfide reverses lung fibrosis in an endothelial AMPK-dependent manner. (a) H_2S synthetase MPST is negatively correlated with fibrotic markers in human fibrotic lungs. The Spearman correlation was performed to analyze the correlation of *MPST* mRNA expression level with fibrotic marker genes (*COL1A1*, *COL3A1*, *CCN2*, *FN1*) mRNA expression level in human lung tissues using the public dataset GSE213001. (b) Design of H_2S-mediated treatment of lung fibrosis in WT mice and mice with endothelial *Prkaa1* knockout. Lung fibrosis in WT mice and mice with endothelial *Prkaa1* knockout was induced with bleomycin, followed by H_2S donor NaHS (10 mg/kg/day) treatment for 21 days. (c) H&E and PSR staining reveal decreased tissue remodeling and collagen deposition in NaHS-treated mice, while this effect is abolished by endothelial-specific *Prkaa1* knockout. (d) Immunofluorescent staining reveals decreased Collagen and αSMA expression in fibrotic lung tissues in NaHS-treated mice, while this effect is abolished by endothelial-specific *Prkaa1* knockout. (e) Measurement of fibrotic marker hydroxyproline in lung tissues shows decreased fibrosis in NaHS-treated mice, while this effect is abolished by endothelial-specific *Prkaa1* knockout (n = 12). (f) Fibrosis-related gene (*Col1a1*, *Col3a1*, *Ctgf*, *Fn1*) expression levels are decreased in NaHS-treated mice, while this effect is abolished by endothelial-specific *Prkaa1* knockout (n = 6).

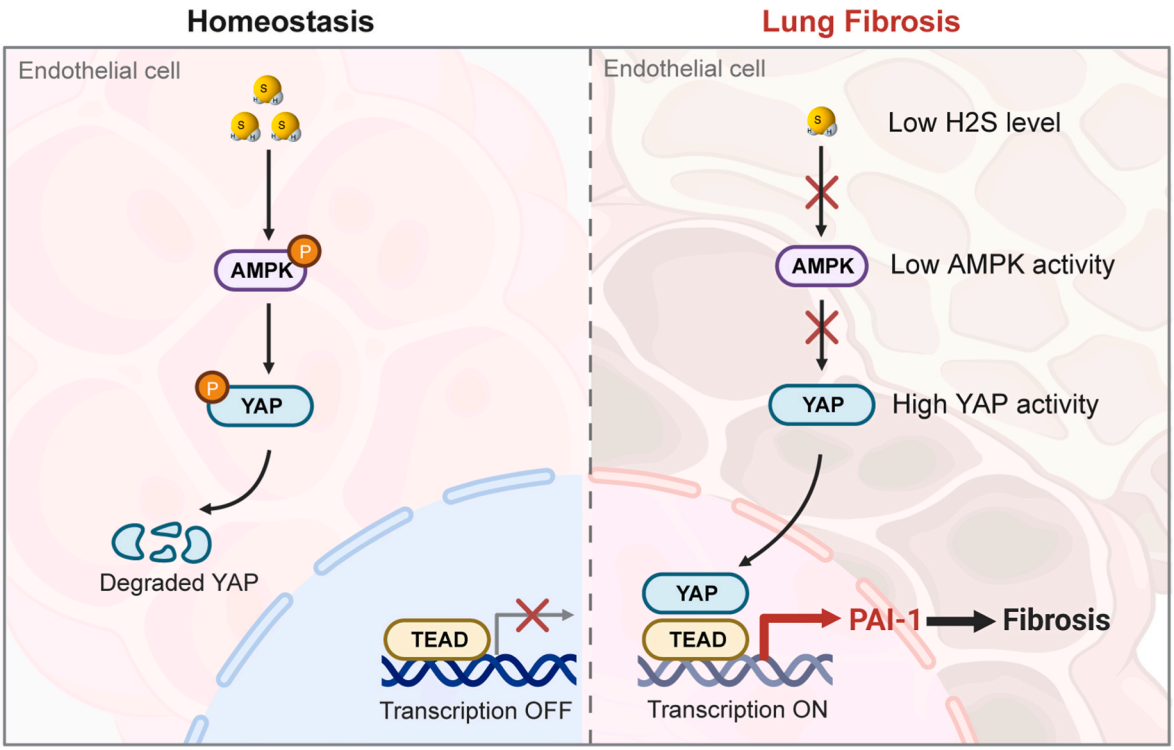

Fig. 7. Endothelial H_2S-AMPK regulates the YAP-PAI-1 axis to participate in lung fibrosis. During lung injury, loss of endogenous H_2S triggers the inactivation of AMPK in endothelial cells. As a result, AMPK fails to induce YAP phosphorylation, leading to the translocation of YAP into the endothelial nucleus, thereby enhancing PAI-1 transcription and subsequently promoting the development of lung fibrosis.

cellular biogenetics, and metabolism regulation [57,62,63]. Previous studies show that H_2S is an endogenous activator for AMPK by targeting mitochondrial electron transport to induce mitochondrial uncoupling [52,53]. In this study, we observed that AMPK inactivation in endothelial cells of fibrotic lungs was partially due to the deficiency of endogenous H_2S. The H_2S synthetase MPST expression level was reduced in endothelial cells, which was coupled with reduced levels of endogenous H_2S in fibrotic lungs. These findings suggest that endothelial H_2S-AMPK is a sensor of fibrotic stress in lung fibrosis and is essentially involved in lung homeostasis and repression of lung fibrosis. Considering the limited number of human samples, which has no sufficient power analysis to demonstrate statistical rigor, these preliminary findings require follow up in larger cohorts before clinical considerations can be made.

H_2S is well known for its antioxidative roles in the cardiovascular system [64]. H_2S can serve as a critical regulator of oxidative stress by directly reacting with reactive oxygen species (ROS) and reactive nitrogen species (RNS), or indirectly through various other mechanisms [55–57,62]. For instance, H_2S can activate classical antioxidants, such as glutathione and the antioxidative transcriptional factor Nrf2 [55–57, 62]. Indeed, the antioxidative roles of H_2S are well-known in preventing fibrosis of multiple organs, including the heart, skeletal muscle, kidney, and liver [64–66]. Notably, H_2S can also reduce ROS production by targeting the mitochondrial respiratory chain and oxidative phosphorylation in the mitochondria, leading to the decline in ATP and subsequently activation of AMPK [52,67,68], which has multiple functions including metabolism regulation and antioxidation [43,69,70]. In this study, we observed that AMPK is a sensor of endogenous H_2S levels and the anti-fibrotic effects of H_2S partially relied on endothelial AMPK in mouse lung fibrosis. These findings further extend our understanding of H_2S in regulating endothelial homeostasis and organ fibrosis [52,54,62, 71–74].

The dysregulation of redox homeostasis in endothelium plays a pivotal role in the pathogenesis of fibrosis partially *via* regulating angiocrine factors [7,12,75,76]. Angiocrine factors derived from endothelial cells play important roles in intercellular communication and are involved in organ development, regeneration, and fibrosis [7]. We observed that AMPK-reregulated multiple HALLMARK gene sets that involved angiocrine factors and we identified PAI-1 as one key downstream effector of AMPK. Our study reveals that PAI-1 is a downstream effector molecule of the endothelial metabolic regulator, AMPK. As a member of the serine protease inhibitor superfamily, PAI-1 regulates fibrinolysis and participates in multiple physiological and pathological processes including cancer, diabetes, cardiovascular diseases, and fibrosis [46,51,77,78]. Notably, PAI-1 controls the activities of urokinase/tissue-type plasminogen activator (uPA/tPA), plasmin, and plasmin-dependent MMPs involved in the proteolytic degradation of ECM proteins. Previous studies have shown that hyperactivation of PAI-1 contributes to excessive ECM deposition during physiological and pathological processes [51,78–80]. In alveolar epithelial type II, PAI-1 contributes to cell senescence by inhibiting P53 degradation in lung fibrosis [44,77]. The coagulation factor PAI-1 is predominantly expressed in fibroblasts/myofibroblasts and endothelial cells in lung tissues (data not shown); thus, endothelial cells may be the predominant source of PAI-1 at the beginning of the fibrotic process whereby endothelial cells have a relative population advantage over fibroblasts/myofibroblasts. We found that PAI-1 was upregulated in endothelial cells of mouse and human fibrotic lung tissues, and PAI-1 was positively correlated with fibrotic gene expression levels in human patients. Fibrosis-induced inhibition of AMPK in endothelial cells leads to overexpression of PAI-1, while PAI-1 inhibitor TPX could alleviate lung fibrosis. Thus, we revealed that endothelial AMPK inactivation promoted profibrotic angiocrine factor PAI-1 expression to accelerate lung fibrosis. However, PAI-1 can regulate tissue homeostasis in coagulation-dependent and independent manners [51]. For instance, recent studies revealed that PAI-1 modulates the immune microenvironment to participate in carcinogenesis [46]. Indeed, our H&E staining showed that PAI-1 inhibitors reduced immune cells in fibrotic lungs, but

further studies are needed to explore the coagulation-dependent and independent roles of PAI-1 in lung fibrosis.

Another interesting finding is the involvement of Hippo in H_2S-AMPK-mediated repression of PAI-1. YAP and the transcriptional co-activator TAZ are the central control modules of the Hippo pathway, which initiates gene expression *via* binding to the TEAD family of transcription factors. As an evolutionarily conserved signaling pathway, the Hippo pathway or YAP/TAZ-TEAD is associated with organ development, homeostasis maintenance, regeneration, wound healing, immune regulation, cancer, and fibrosis [81,82]. AMPK has been reported to modulate the phosphorylation of YAP and inhibit YAP transcription activity directly upon metabolic stress [48–50]. Notably, our studies showed that endothelial inactivation of AMPK led to YAP hypophosphorylation/activation in fibrotic lungs. Utilizing ChIP-seq analysis, we found transcription complex YAP/TAZ-TEAD binds to the transcription start site of *SERPINE1* in human endothelial cells. Inhibition or knockdown of YAP decreases *SERPINE1* expression. These results highlight the role of the endothelial AMPK-YAP-PAI-1 axis in fibrotic lungs. Our recent study also demonstrated that YAP regulates the immune response in macrophages to modulate the immune microenvironment and organ fibrosis [19]. Thus, the Hippo pathway is critically involved in organ fibrosis through the regulation of multiple cell types, including endothelial cells and macrophages. The Hippo pathway plays multiple roles in lung homeostasis. Our findings suggest that endothelial Hippo may promote lung fibrosis by partially regulating the angiocrine factor PAI-1. Interestingly, Hippo in epithelial and endothelial cells is essential for lung development and alveolar regeneration [83–85]. Thus, the Hippo pathway may play complicated roles at different stages and in different cell types during lung injury, regeneration, and fibrosis. In addition, YAP and its subcellular localization have distinct compartment-specific roles in developing lungs [86], which may explain its complicated functions. Given these facts, accurately targeting the Hippo pathway to promote regeneration and repress fibrosis is tricky, but cell-type specific YAP inhibitors may be a good option, as we have provided recently [19].

Taken together, our study suggests that the endothelial H_2S-AMPK axis is a sensor of fibrotic risk, and dysfunction of this sensor upregulates the anti-fibrinolytic factor PAI-1 *via* activating YAP and contributes to lung fibrosis. This study may provide an elucidation by which endothelial cells sense fibrotic stress to trigger pro-fibrotic angiocrine factors. This endothelial signaling axis may be a potential target for treating lung fibrosis.

CRediT authorship contribution statement

Xiangqi Chen: Data curation, Formal analysis, Investigation, Methodology, Validation, Visualization, Writing – original draft, Writing – review & editing. **Han Wang:** Formal analysis, Validation. **Chuan Wu:** Formal analysis, Validation. **Xiaoyan Li:** Data curation. **Xiaojuan Huang:** Resources. **Yafeng Ren:** Resources. **Qiang Pu:** Resources. **Zhongwei Cao:** Conceptualization, Funding acquisition. **Xiaoqiang Tang:** Conceptualization, Data curation, Funding acquisition, Supervision, Writing – review & editing. **Bi-Sen Ding:** Conceptualization, Data curation, Funding acquisition, Project administration, Supervision, Writing – review & editing.

Declaration of competing interest

The authors declare that they have no conflict of interest.

Data availability

The raw and processed data of RNA-seq have been deposited in the NCBI Gene Expression Omnibus (GEO) database (GSE250474).

Acknowledgments

The authors thank members of Ding lab for constructive discussion. This study was supported by the National Natural Science Foundation of China (81925005, 81970426, 82125002, 92268201, U21A20333).

Appendix A. Supplementary data

Supplementary data to this article can be found online at https://doi.org/10.1016/j.redox.2024.103038.

References

[1] X. Zhao, J.Y.Y. Kwan, K. Yip, P.P. Liu, F.F. Liu, Targeting metabolic dysregulation for fibrosis therapy, Nat. Rev. Drug Discov. 19 (2020) 57–75.
[2] N.C. Henderson, F. Rieder, T.A. Wynn, Fibrosis: from mechanisms to medicines, Nature 587 (2020) 555–566.
[3] T. Koudstaal, M. Funke-Chambour, M. Kreuter, P.L. Molyneaux, M.S. Wijsenbeek, Pulmonary fibrosis: from pathogenesis to clinical decision-making, Trends Mol. Med. 29 (2023) 1076–1087.
[4] G.Y. Liu, G.R.S. Budinger, J.E. Dematte, Advances in the management of idiopathic pulmonary fibrosis and progressive pulmonary fibrosis, BMJ 377 (2022) e066354.
[5] T. Karampitsakos, B.M. Juan-Guardela, A. Tzouvelekis, J.D. Herazo-Maya, Precision medicine advances in idiopathic pulmonary fibrosis, EBioMedicine 95 (2023) 104766.
[6] I. Borek, A. Birnhuber, N.F. Voelkel, L.M. Marsh, G. Kwapiszewska, The vascular perspective on acute and chronic lung disease, J. Clin. Investig. 133 (2023) e170502.
[7] S. Rafii, J.M. Butler, B.S. Ding, Angiocrine functions of organ-specific endothelial cells, Nature 529 (2016) 316–325.
[8] C. Ottone, B. Krusche, A. Whitby, M. Clements, G. Quadrato, M.E. Pitulescu, R. H. Adams, S. Parrinello, Direct cell-cell contact with the vascular niche maintains quiescent neural stem cells, Nat. Cell Biol. 16 (2014) 1045–1056.
[9] J.H. Lee, D.H. Bhang, A. Beede, T.L. Huang, B.R. Stripp, K.D. Bloch, A.J. Wagers, Y. H. Tseng, S. Ryeom, C.F. Kim, Lung stem cell differentiation in mice directed by endothelial cells via a BMP4-NFATc1-thrombospondin-1 axis, Cell 156 (2014) 440–455.
[10] S. Rafii, Z. Cao, R. Lis, Siempos II, D. Chavez, K. Shido, S.Y. Rabbany, B.S. Ding, Platelet-derived SDF-1 primes the pulmonary capillary vascular niche to drive lung alveolar regeneration, Nat. Cell Biol. 17 (2015) 123–136.
[11] B.S. Ding, Z. Cao, R. Lis, D.J. Nolan, P. Guo, M. Simons, M.E. Penfold, K. Shido, S. Y. Rabbany, S. Rafii, Divergent angiocrine signals from vascular niche balance liver regeneration and fibrosis, Nature 505 (2014) 97–102.
[12] J.M. Gomez-Salinero, T. Itkin, S. Rafii, Developmental angiocrine diversification of endothelial cells for organotypic regeneration, Dev. Cell 56 (2021) 3042–3051.
[13] Y. Chen, Q. Pu, Y. Ma, H. Zhang, T. Ye, C. Zhao, X. Huang, Y. Ren, L. Qiao, H. M. Liu, C.T. Esmon, B.S. Ding, Z. Cao, Aging reprograms the hematopoietic-vascular niche to impede regeneration and promote fibrosis, Cell Metabol. 33 (2021) 395–410 e394.
[14] H. Zhang, Y. Ma, X. Cheng, D. Wu, X. Huang, B. Chen, Y. Ren, W. Jiang, X. Tang, T. Bai, Y. Chen, Y. Zhao, C. Zhang, X. Xiao, J. Liu, Y. Deng, T. Ye, L. Chen, H.M. Liu, S.L. Friedman, L. Chen, B.S. Ding, Z. Cao, Targeting epigenetically maladapted vascular niche alleviates liver fibrosis in nonalcoholic steatohepatitis, Sci. Transl. Med. 13 (2021) eabd1206.
[15] T. Yanagihara, K. Tsubouchi, Q. Zhou, M. Chong, K. Otsubo, T. Isshiki, J.C. Schupp, S. Sato, C. Scallan, C. Upagupta, S. Revill, A. Ayoub, S.G. Chong, A. Dvorkin-Gheva, N. Kaminski, J. Tikkanen, S. Keshavjee, G. Pare, C. Guignabert, K. Ask, M.R.J. Kolb, Vascular-parenchymal cross-talk promotes lung fibrosis through BMPR2 signaling, Am. J. Respir. Crit. Care Med. 207 (2023) 1498–1514.
[16] Z. Cao, R. Lis, M. Ginsberg, D. Chavez, K. Shido, S.Y. Rabbany, G.H. Fong, T. P. Sakmar, S. Rafii, B.S. Ding, Targeting of the pulmonary capillary vascular niche promotes lung alveolar repair and ameliorates fibrosis, Nat. Med. 22 (2016) 154–162.
[17] B.S. Ding, D.J. Nolan, P. Guo, A.O. Babazadeh, Z. Cao, Z. Rosenwaks, R.G. Crystal, M. Simons, T.N. Sato, S. Worgall, K. Shido, S.Y. Rabbany, S. Rafii, Endothelial-derived angiocrine signals induce and sustain regenerative lung alveolarization, Cell 147 (2011) 539–553.
[18] H. Zhang, Y. Ma, X. Cheng, D. Wu, X. Huang, B. Chen, Y. Ren, W. Jiang, X. Tang, T. Bai, Y. Chen, Y. Zhao, C. Zhang, X. Xiao, J. Liu, Y. Deng, T. Ye, L. Chen, H.M. Liu, S.L. Friedman, L. Chen, B.S. Ding, Z. Cao, Targeting epigenetically maladapted vascular niche alleviates liver fibrosis in nonalcoholic steatohepatitis, Sci. Transl. Med. 13 (2021) eabd1206.
[19] J. Qing, Y. Ren, Y. Zhang, M. Yan, H. Zhang, D. Wu, Y. Ma, Y. Chen, X. Huang, Q. Wu, M. Mazhar, L. Wang, J. Liu, B.S. Ding, Z. Cao, Dopamine receptor D2 antagonism normalizes profibrotic macrophage-endothelial crosstalk in non-alcoholic steatohepatitis, J. Hepatol. 76 (2022) 394–406.
[20] J.L. Duan, J.J. Liu, B. Ruan, J. Ding, Z.Q. Fang, H. Xu, P. Song, C. Xu, Z.W. Li, W. Du, M. Xu, Y.W. Ling, F. He, L. Wang, Age-related liver endothelial zonation triggers steatohepatitis by inactivating pericentral endothelium-derived C-kit, Nat Aging 3 (2023) 258–274.
[21] J.U.G. Wagner, L.S. Tombor, P.F. Malacarne, L.M. Kettenhausen, J. Panthel, H. Kujundzic, N. Manickam, K. Schmitz, M. Cipca, K.A. Stilz, A. Fischer, M. Muhly-

Reinholz, W.T. Abplanalp, D. John, S.K. Mohanta, C. Weber, A.J.R. Habenicht, G. K. Buchmann, S. Angendohr, E. Amin, K. Scherschel, N. Klöcker, M. Kelm, D. Schüttler, S. Clauss, S. Günther, T. Boettger, T. Braun, C. Bär, M.D. Pham, J. Krishnan, S. Hille, O.J. Müller, T. Bozoglu, C. Kupatt, E. Nardini, S. Osmanagic-Myers, C. Meyer, A.M. Zeiher, R.P. Brandes, G. Luxán, S. Dimmeler, Aging impairs the neurovascular interface in the heart, Science 381 (2023) 897–906.

[22] Y. Cao, Y. Wang, Z. Zhou, C. Pan, L. Jiang, Z. Zhou, Y. Meng, S. Charugundla, T. Li, H. Allayee, M.M. Seldin, A.J. Lusis, Liver-heart cross-talk mediated by coagulation factor XI protects against heart failure, Science 377 (2022) 1399–1406.

[23] X. Tang, Y.X. Luo, H.Z. Chen, D.P. Liu, Mitochondria, endothelial cell function, and vascular diseases, Front. Physiol. 5 (2014) 175.

[24] X. Sun, Y. Zhang, X.-F. Chen, X. Tang, Acylations in cardiovascular biology and diseases, what's beyond acetylation, EBioMedicine 67 (2023) 104418.

[25] X. Li, X. Sun, P. Carmeliet, Hallmarks of endothelial cell metabolism in health and disease, Cell Metabol. 30 (2019) 414–433.

[26] G. Eelen, P.d. Zeeuw, L. Treps, U. Harjes, B.W. Wong, P. Carmeliet, Endothelial cell metabolism, Physiol. Rev. 98 (2018) 3–58.

[27] I.A. Tamargo, K.I. Baek, Y. Kim, C. Park, H. Jo, Flow-induced reprogramming of endothelial cells in atherosclerosis, Nat. Rev. Cardiol. 20 (2023) 738–753.

[28] G.R. Steinberg, D.G. Hardie, New insights into activation and function of the AMPK, Nat. Rev. Mol. Cell Biol. 24 (2023) 255–272.

[29] D. Wu, D. Hu, H. Chen, G. Shi, I.S. Fetahu, F. Wu, K. Rabidou, R. Fang, L. Tan, S. Xu, H. Liu, C. Argueta, L. Zhang, F. Mao, G. Yan, J. Chen, Z. Dong, R. Lv, Y. Xu, M. Wang, Y. Ye, S. Zhang, D. Duquette, S. Geng, C. Yin, C.G. Lian, G.F. Murphy, G. K. Adler, R. Garg, L. Lynch, P. Yang, Y. Li, F. Lan, J. Fan, Y. Shi, Y.G. Shi, Glucose-regulated phosphorylation of TET2 by AMPK reveals a pathway linking diabetes to cancer, Nature 559 (2018) 637–641.

[30] S. Chen, X. Liu, C. Peng, C. Tan, H. Sun, H. Liu, Y. Zhang, P. Wu, C. Cui, C. Liu, D. Yang, Z. Li, J. Lu, J. Guan, X. Ke, R. Wang, X. Bo, X. Xu, J. Han, J. Liu, The phytochemical hyperforin triggers thermogenesis in adipose tissue via a Dlat-AMPK signaling axis to curb obesity, Cell Metabol. 33 (2021) 565–580 e567.

[31] P. Zhao, X. Sun, C. Chaggan, Z. Liao, K. In Wong, F. He, S. Singh, R. Loomba, M. Karin, J.L. Witztum, A.R. Saltiel, An AMPK-caspase-6 axis controls liver damage in nonalcoholic steatohepatitis, Science 367 (2020) 652–660.

[32] S. Rangarajan, N.B. Bone, A.A. Zmijewska, S. Jiang, D.W. Park, K. Bernard, M. L. Locy, S. Ravi, J. Deshane, R.B. Mannon, E. Abraham, V. Darley-Usmar, V. J. Thannickal, J.W. Zmijewski, Metformin reverses established lung fibrosis in a bleomycin model, Nat. Med. 24 (2018) 1121–1127.

[33] Y. Han, M. He, T. Marin, H. Shen, W.T. Wang, T.Y. Lee, H.C. Hong, Z.L. Jiang, T. Garland Jr., J.Y. Shyy, B. Gongol, S. Chien, Roles of KLF4 and AMPK in the inhibition of glycolysis by pulsatile shear stress in endothelial cells, Proc. Natl. Acad. Sci. U. S. A. 118 (2021) e2103982118.

[34] Q. Yang, J. Xu, Q. Ma, Z. Liu, V. Sudhahar, Y. Cao, L. Wang, X. Zeng, Y. Zhou, M. Zhang, Y. Xu, Y. Wang, N.L. Weintraub, C. Zhang, T. Fukai, C. Wu, L. Huang, Z. Han, T. Wang, D.J. Fulton, M. Hong, Y. Huo, PRKAA1/AMPKα1-driven glycolysis in endothelial cells exposed to disturbed flow protects against atherosclerosis, Nat. Commun. 9 (2018) 4667.

[35] C. Rutherford, C. Speirs, J.J. Williams, M.A. Ewart, S.J. Mancini, S.A. Hawley, C. Delles, B. Viollet, A.P. Costa-Pereira, G.S. Baillie, I.P. Salt, T.M. Palmer, Phosphorylation of Janus kinase 1 (JAK1) by AMP-activated protein kinase (AMPK) links energy sensing to anti-inflammatory signaling, Sci. Signal. 9 (2016) ra109.

[36] J. Zhang, J. Dong, M. Martin, M. He, B. Gongol, T.L. Marin, L. Chen, X. Shi, Y. Yin, F. Shang, Y. Wu, H.Y. Huang, J. Zhang, Y. Zhang, J. Kang, E.A. Moya, H.D. Huang, F.L. Powell, Z. Chen, P.A. Thistlethwaite, Z.Y. Yuan, J.Y. Shyy, AMP-activated protein kinase phosphorylation of angiotensin-converting enzyme 2 in endothelium mitigates pulmonary hypertension, Am. J. Respir. Crit. Care Med. 198 (2018) 509–520.

[37] W. Zhang, Q. Wang, Y. Wu, C. Moriasi, Z. Liu, X. Dai, Q. Wang, W. Liu, Z.Y. Yuan, M.H. Zou, Endothelial cell-specific liver kinase B1 deletion causes endothelial dysfunction and hypertension in mice in vivo, Circulation 129 (2014) 1428–1439.

[38] H. Shen, J. Zhang, C. Wang, P.P. Jain, M. Xiong, X. Shi, Y. Lei, S. Chen, Q. Yin, P. A. Thistlethwaite, J. Wang, K. Gong, Z.Y. Yuan, J.X. Yuan, J.Y. Shyy, MDM2-mediated ubiquitination of angiotensin-converting enzyme 2 contributes to the development of pulmonary arterial hypertension, Circulation 142 (2020) 1190–1204.

[39] F.Y. Li, K.S. Lam, H.F. Tse, C. Chen, Y. Wang, P.M. Vanhoutte, A. Xu, Endothelium-selective activation of AMP-activated protein kinase prevents diabetes mellitus-induced impairment in vascular function and reendothelialization via induction of heme oxygenase-1 in mice, Circulation 126 (2012) 1267–1277.

[40] C.C. Thornton, F. Al-Rashed, D. Calay, G.M. Birdsey, A. Bauer, H. Mylroie, B. J. Morley, A.M. Randi, D.O. Haskard, J.J. Boyle, J.C. Mason, Methotrexate-mediated activation of an AMPK-CREB-dependent pathway: a novel mechanism for vascular protection in chronic systemic inflammation, Ann. Rheum. Dis. 75 (2016) 439–448.

[41] J.Y. Luo, C.K. Cheng, L. He, Y. Pu, Y. Zhang, X. Lin, A. Xu, C.W. Lau, X.Y. Tian, R.C. W. Ma, H. Jo, Y. Huang, Endothelial UCP2 is a mechanosensitive suppressor of atherosclerosis, Circ. Res. 131 (2022) 424–441.

[42] X. Lin, B. Swedlund, M.N. Ton, S. Ghazanfar, C. Guibentif, C. Paulissen, E. Baudelet, E. Plaindoux, Y. Achouri, E. Calonne, C. Dubois, W. Mansfield, S. Zaffran, J.C. Marioni, F. Fuks, B. Gottgens, F. Lescroart, C. Blanpain, Mesp1 controls the chromatin and enhancer landscapes essential for spatiotemporal patterning of early cardiovascular progenitors, Nat. Cell Biol. 24 (2022) 1114–1128.

[43] S. Herzig, R.J. Shaw, AMPK: guardian of metabolism and mitochondrial homeostasis, Nat. Rev. Mol. Cell Biol. 19 (2018) 121–135.

[44] C. Jiang, G. Liu, L. Cai, J. Deshane, V. Antony, V.J. Thannickal, R.M. Liu, Divergent regulation of alveolar Type 2 cell and fibroblast apoptosis by plasminogen activator inhibitor 1 in lung fibrosis, Am. J. Pathol. 191 (2021) 1227–1239.

[45] S.S. Khan, S.J. Shah, J.L. Strande, A.S. Baldridge, P. Flevaris, M.J. Puckelwartz, E. M. McNally, L.J. Rasmussen-Torvik, D.C. Lee, J.C. Carr, B.C. Benefield, M.Z. Afzal, M. Heiman, S. Gupta, A.D. Shapiro, D.E. Vaughan, Identification of cardiac fibrosis in young adults with a homozygous frameshift variant in SERPINE1, JAMA Cardiology 6 (2021) 841–846.

[46] J. Dong, C. Zhu, Y. Huang, Q. Li, J. Li, Z. Wang, Y. Wang, Z. Zhou, M. Sun, Reversing the PAI-1-induced fibrotic immune exclusion of solid tumor by multivalent CXCR4 antagonistic nano-permeator, Acta Pharm. Sin. B 13 (2023) 3106–3120.

[47] I.M. Moya, G. Halder, Hippo-YAP/TAZ signalling in organ regeneration and regenerative medicine, Nat. Rev. Mol. Cell Biol. 20 (2019) 211–226.

[48] W. Wang, Z.D. Xiao, X. Li, K.E. Aziz, B. Gan, R.L. Johnson, J. Chen, AMPK modulates Hippo pathway activity to regulate energy homeostasis, Nat. Cell Biol. 17 (2015) 490–499.

[49] M. DeRan, J. Yang, C.H. Shen, E.C. Peters, J. Fitamant, P. Chan, M. Hsieh, S. Zhu, J. M. Asara, B. Zheng, N. Bardeesy, J. Liu, X. Wu, Energy stress regulates Hippo-YAP signaling involving AMPK-mediated regulation of angiomotin-like 1 protein, Cell Rep. 9 (2014) 495–503.

[50] J.S. Mo, Z. Meng, Y.C. Kim, H.W. Park, C.G. Hansen, S. Kim, D.S. Lim, K.L. Guan, Cellular energy stress induces AMPK-mediated regulation of YAP and the Hippo pathway, Nat. Cell Biol. 17 (2015) 500–510.

[51] W. Dai, H. Zhang, H. Lund, Z. Zhang, M. Castleberry, M. Rodriguez, G. Kuriakose, S. Gupta, M. Lewandowska, H.R. Powers, S. Valmiki, J. Zhu, A.D. Shapiro, M. M. Hussain, J.A. López, M.G. Sorci-Thomas, R.L. Silverstein, H.N. Ginsberg, D. Sahoo, I. Tabas, Z. Zheng, Intracellular tPA-PAI-1 interaction determines VLDL assembly in hepatocytes, Science 381 (2023) eadh5207.

[52] A. Longchamp, T. Mirabella, A. Arduini, M.R. MacArthur, A. Das, J.H. Trevino-Villarreal, C. Hine, I. Ben-Sahra, N.H. Knudsen, L.E. Brace, J. Reynolds, P. Mejia, M. Tao, G. Sharma, R. Wang, J.M. Corpataux, J.A. Haefliger, K.H. Ahn, C.H. Lee, B. D. Manning, D.A. Sinclair, C.S. Chen, C.K. Ozaki, J.R. Mitchell, Amino acid restriction triggers angiogenesis via GCN2/ATF4 regulation of VEGF and H(2)S production, Cell 173 (2018) 117–129 e114.

[53] J. Jia, Z. Wang, M. Zhang, C. Huang, Y. Song, F. Xu, J. Zhang, J. Li, M. He, Y. Li, G. Ao, C. Hong, Y. Cao, Y.E. Chin, Z.-c. Hua, J. Cheng, SQR mediates therapeutic effects of H_2S by targeting mitochondrial electron transport to induce mitochondrial uncoupling, Sci. Adv. 6 (2020) eaaz5752.

[54] A. Das, G.X. Huang, M.S. Bonkowski, A. Longchamp, C. Li, M.B. Schultz, L.J. Kim, B. Osborne, S. Joshi, Y. Lu, J.H. Trevino-Villarreal, M.J. Kang, T.T. Hung, B. Lee, E. O. Williams, M. Igarashi, J.R. Mitchell, L.E. Wu, N. Turner, Z. Arany, L. Guarente, D.A. Sinclair, Impairment of an endothelial NAD(+)-H(2)S signaling network is a reversible cause of vascular aging, Cell 176 (2018) 74–89.

[55] S. Rajpal, P. Katikaneni, M. Deshotels, S. Pardue, J. Glawe, X. Shen, N. Akkus, K. Modi, R. Bhandari, P. Dominic, P. Reddy, G.K. Kolluru, C.G. Kevil, Total sulfane sulfur bioavailability reflects ethnic and gender disparities in cardiovascular disease, Redox Biol. 15 (2018) 480–489.

[56] M. Watts, G.K. Kolluru, P. Dherange, S. Pardue, M. Si, X. Shen, K. Trosclair, J. Glawe, Z. Al-Yafeai, M. Iqbal, B.H. Pearson, K.A. Hamilton, A.W. Orr, E. Glasscock, C.G. Kevil, P. Dominic, Decreased bioavailability of hydrogen sulfide links vascular endothelium and atrial remodeling in atrial fibrillation, Redox Biol. 38 (2021) 101817.

[57] G. Cirino, C. Szabo, A. Papapetropoulos, Physiological roles of hydrogen sulfide in mammalian cells, tissues, and organs, Physiol. Rev. 103 (2023) 31–276.

[58] X. Tang, X.F. Chen, N.Y. Wang, X.M. Wang, S.T. Liang, W. Zheng, Y.B. Lu, X. Zhao, D.L. Hao, Z.Q. Zhang, M.H. Zou, D.P. Liu, H.Z. Chen, SIRT2 acts as a cardioprotective deacetylase in pathological cardiac hypertrophy, Circulation 136 (2017) 2051–2067.

[59] H. Gong, H. Chen, P. Xiao, N. Huang, X. Han, J. Zhang, Y. Yang, T. Li, T. Zhao, H. Tai, W. Xu, G. Zhang, C. Gong, M. Yang, X. Tang, H. Xiao, miR-146a impedes the anti-aging effect of AMPK via NAMPT suppression and NAD^+/SIRT inactivation, Signal Transduct. Targeted Ther. 7 (2022) 66.

[60] D.A. Landry, E. Yakubovich, D.P. Cook, S. Fasih, J. Upham, B.C. Vanderhyden, Metformin prevents age-associated ovarian fibrosis by modulating the immune landscape in female mice, Sci. Adv. 8 (2022) eabq1475.

[61] V. Kheirollahi, R.M. Wasnick, V. Biasin, A.I. Vazquez-Armendariz, X. Chu, A. Moiseenko, A. Weiss, J. Wilhelm, J.S. Zhang, G. Kwapiszewska, S. Herold, R. T. Schermuly, B. Mari, X. Li, W. Seeger, A. Günther, S. Bellusci, E. El Agha, Metformin induces lipogenic differentiation in myofibroblasts to reverse lung fibrosis, Nat. Commun. 10 (2019) 2987.

[62] G.K. Kolluru, R.E. Shackelford, X. Shen, P. Dominic, C.G. Kevil, Sulfide regulation of cardiovascular function in health and disease, Nat. Rev. Cardiol. 20 (2023) 109–125.

[63] Y. Chen, C.G. Kevil, Redox signaling and cardiovascular disease: new paradigms and discoveries, Redox Biol. 37 (2020) 101743.

[64] Z. Li, D.J. Polhemus, D.J. Lefer, Evolution of hydrogen sulfide therapeutics to treat cardiovascular disease, Circ. Res. 123 (2018) 590–600.

[65] H.-J. Sun, Z.-Y. Wu, X.-W. Nie, X.-Y. Wang, J.-S. Bian, Implications of hydrogen sulfide in liver pathophysiology: Mechanistic insights and therapeutic potential, J. Adv. Res. 27 (2021) 127–135.

[66] Z. Li, H. Xia, T.E. Sharp, K.B. LaPenna, A. Katsouda, J.W. Elrod, J. Pfeilschifter, K.-F. Beck, S. Xu, M. Xian, T.T. Goodchild, A. Papapetropoulos, D.J. Lefer, Hydrogen sulfide modulates endothelial–mesenchymal transition in heart failure, Circ. Res. 132 (2023) 154–166.

[67] B. Murphy, R. Bhattacharya, P. Mukherjee, Hydrogen sulfide signaling in mitochondria and disease, Faseb. J. 33 (2019) 13098–13125.
[68] U. Karunakaran, S. Elumalai, S.M. Chung, K. Maedler, K.C. Won, J.S. Moon, Mitochondrial aldehyde dehydrogenase-2 coordinates the hydrogen sulfide - AMPK axis to attenuate high glucose-induced pancreatic β-cell dysfunction by glutathione antioxidant system, Redox Biol. (2023) 102994.
[69] C. Mo, L. Wang, J. Zhang, S. Numazawa, H. Tang, X. Tang, X. Han, J. Li, M. Yang, Z. Wang, D. Wei, H. Xiao, The crosstalk between Nrf2 and AMPK signal pathways is important for the anti-inflammatory effect of berberine in LPS-stimulated macrophages and endotoxin-shocked mice, Antioxidants Redox Signal. 20 (2014) 574–588.
[70] P. Sekar, G. Hsiao, S.-H. Hsu, D.-Y. Huang, W.-W. Lin, C.-M. Chan, Metformin inhibits methylglyoxal-induced retinal pigment epithelial cell death and retinopathy via AMPK-dependent mechanisms: Reversing mitochondrial dysfunction and upregulating glyoxalase 1, Redox Biol. 64 (2023) 102786.
[71] R. Wang, C. Szabo, F. Ichinose, A. Ahmed, M. Whiteman, A. Papapetropoulos, The role of H2S bioavailability in endothelial dysfunction, Trends Pharmacol. Sci. 36 (2015) 568–578.
[72] G. Yang, L. Wu, B. Jiang, W. Yang, J. Qi, K. Cao, Q. Meng, A.K. Mustafa, W. Mu, S. Zhang, S.H. Snyder, R. Wang, H2S as a physiologic vasorelaxant: hypertension in mice with deletion of cystathionine gamma-lyase, Science 322 (2008) 587–590.
[73] S. Alam, S. Pardue, X. Shen, J.D. Glawe, T. Yagi, M.A.N. Bhuiyan, R.P. Patel, P. S. Dominic, C.S. Virk, M.S. Bhuiyan, A.W. Orr, C. Petit, G.K. Kolluru, C.G. Kevil, Hypoxia increases persulfide and polysulfide formation by AMP kinase dependent cystathionine gamma lyase phosphorylation, Redox Biol. 68 (2023) 102949.
[74] S.C. Bir, C.G. Kevil, Sulfane sustains vascular health: insights into cystathionine γ-lyase function, Circulation 127 (2013) 2472–2474.
[75] M. Ruart, L. Chavarria, G. Camprecios, N. Suarez-Herrera, C. Montironi, S. Guixe-Muntet, J. Bosch, S.L. Friedman, J.C. Garcia-Pagan, V. Hernandez-Gea, Impaired endothelial autophagy promotes liver fibrosis by aggravating the oxidative stress response during acute liver injury, J. Hepatol. 70 (2019) 458–469.
[76] V. Anathy, K.G. Lahue, D.G. Chapman, S.B. Chia, D.T. Casey, R. Aboushousha, J.L. J. van der Velden, E. Elko, S.M. Hoffman, D.H. McMillan, J.T. Jones, J.D. Nolin, S. Abdalla, R. Schneider, D.J. Seward, E.C. Roberson, M.D. Liptak, M.E. Cousins, K. J. Butnor, D.J. Taatjes, R.C. Budd, C.G. Irvin, Y.S. Ho, R. Hakem, K.K. Brown, R. Matsui, M.M. Bachschmid, J.L. Gomez, N. Kaminski, A. van der Vliet, Y.M. W. Janssen-Heininger, Reducing protein oxidation reverses lung fibrosis, Nat. Med. 24 (2018) 1128–1135.
[77] C. Jiang, G. Liu, T. Luckhardt, V. Antony, Y. Zhou, A.B. Carter, V.J. Thannickal, R. M. Liu, Serpine 1 induces alveolar type II cell senescence through activating p53-p21-Rb pathway in fibrotic lung disease, Aging Cell 16 (2017) 1114–1124.
[78] Y. Qin, J. Zhang, S. Babapoor-Farrokhran, B. Applewhite, M. Deshpande, H. Megarity, M. Flores-Bellver, S. Aparicio-Domingo, T. Ma, Y. Rui, S.Y. Tzeng, J. J. Green, M.V. Canto-Soler, S. Montaner, A. Sodhi, PAI-1 is a vascular cell-specific HIF-2-dependent angiogenic factor that promotes retinal neovascularization in diabetic patients, Sci. Adv. 8 (2022) eabm1896.
[79] L. Liberale, Y.M. Puspitasari, S. Ministrini, A. Akhmedov, S. Kraler, N.R. Bonetti, G. Beer, A. Vukolic, D. Bongiovanni, J. Han, K. Kirmes, I. Bernlochner, J. Pelisek, J. H. Beer, Z.G. Jin, D. Pedicino, G. Liuzzo, K. Stellos, F. Montecucco, F. Crea, T. F. Lüscher, G.G. Camici, JCAD promotes arterial thrombosis through PI3K/Akt modulation: a translational study, Eur. Heart J. 44 (2023) 1818–1833.
[80] S. Kang, T. Tanaka, H. Inoue, C. Ono, S. Hashimoto, Y. Kioi, H. Matsumoto, H. Matsuura, T. Matsubara, K. Shimizu, H. Ogura, Y. Matsuura, T. Kishimoto, IL-6 trans-signaling induces plasminogen activator inhibitor-1 from vascular endothelial cells in cytokine release syndrome, Proc. Natl. Acad. Sci. U. S. A. 117 (2020) 22351–22356.
[81] A. Dey, X. Varelas, K.L. Guan, Targeting the Hippo pathway in cancer, fibrosis, wound healing and regenerative medicine, Nat. Rev. Drug Discov. 19 (2020) 480–494.
[82] J.M. Franklin, Z. Wu, K.L. Guan, Insights into recent findings and clinical application of YAP and TAZ in cancer, Nat. Rev. Cancer 23 (2023) 512–525.
[83] G.T. DiGiovanni, W. Han, T.P. Sherrill, C.J. Taylor, D.S. Nichols, N.M. Geis, U. K. Singha, C.L. Calvi, A.S. McCall, M.M. Dixon, Y. Liu, J.H. Jang, S.S. Gutor, V. V. Polosukhin, T.S. Blackwell, J.A. Kropski, J.J. Gokey, Epithelial Yap/Taz are required for functional alveolar regeneration following acute lung injury, JCI Insight 8 (2023) e173374.
[84] T. Mammoto, M. Muyleart, A. Mammoto, Endothelial YAP1 in regenerative lung growth through the angiopoietin-Tie2 pathway, Am. J. Respir. Cell Mol. Biol. 60 (2019) 117–127.
[85] Z. Liu, H. Wu, K. Jiang, Y. Wang, W. Zhang, Q. Chu, J. Li, H. Huang, T. Cai, H. Ji, C. Yang, N. Tang, MAPK-mediated YAP activation controls mechanical-tension-induced pulmonary alveolar regeneration, Cell Rep. 16 (2016) 1810–1819.
[86] B.J. van Soldt, J. Qian, J. Li, N. Tang, J. Lu, W.V. Cardoso, Yap and its subcellular localization have distinct compartment-specific roles in the developing lung, Development 146 (2019) dev175810.